International Journal of Solids and Structures 50 (2013) 609–622

Contents lists available at SciVerse ScienceDirect

International Journal of Solids and Structures

journal homepage: www.elsevier.com/locate/ijsolstr

Semi-analytical method for computing effective properties in elastic composite under imperfect contact

José A. Otero [a,*], Reinaldo Rodríguez-Ramos [b], Julián Bravo-Castillero [b], Raúl Guinovart-Díaz [b], Federico J. Sabina [c], G. Monsivais [d]

[a] Instituto de Cibernética, Matemática y Física (ICIMAF), Calle 15 No. 551, entre C y D, Vedado, Habana 4, CP 10400, Cuba
[b] Facultad de Matemática y Computación, Universidad de la Habana, San Lázaro y L, Vedado, Habana 4, CP 10400, Cuba
[c] Instituto de Investigaciones en Matemáticas Aplicadas y en Sistemas, Universidad Nacional Autónoma de México, Apartado Postal 20-726, Delegación de Alvaro Obregón, 01000 México D.F., Mexico
[d] Instituto de Física, Universidad Nacional Autónoma de México, Apartado Postal 20-364, 01000 México D.F., Mexico

ARTICLE INFO

Article history:
Received 3 February 2012
Received in revised form 21 September 2012
Available online 15 November 2012

Keywords:
Fiber-reinforced composites
Asymptotic homogenization method
Finite element method
Effective properties
Imperfect adhesion
Imperfect elastic composites

ABSTRACT

A parallel fiber-reinforced periodic elastic composite is considered with transversely iso-tropic constituents. Fibers with circular cross section are distributed with the same periodicity along the two perpendicular directions to the fiber orientation, i.e., the periodic cell of the composite is square. The composite exhibits imperfect contact, in particular, spring type at the interface between the fiber and matrix is modeled. Effective properties of this composite for in-plane and anti-plane local problems are calculated by means of a semi-analytic method, i.e. the differential equations that described the local problems obtained by asymptotic homogenization method are solved using the finite element method. Numerical computations are implemented and comparisons with exact solutions are presented.

1. Introduction

In most composites, the fiber-matrix adhesion is imperfect, i.e., the continuity conditions for stresses and displacements are not satisfied. Thus, various approaches have been used, where the bond between the reinforcement and the matrix is modeled by an interphase with specified thickness (Hashin, 2002; Guinovart-Diaz et al., 2005). Other assumptions suppose that the contrast or jump of the displacements in the interface is proportional to the corresponding component of the traction in the interface in terms of a parameter given by the spring constant (imperfect parameters). This type of imperfect contact (spring type) in the interphases of the composites was investigated by Jasiuk and Tong (1989), Hashin (1990), Achenbach and Zhu (1990), Hashin (1991a,b) and Lopez-Realpozo et al. (2011). Hashin has derived the connection between the parameters of sprint type interface and the properties of an isotropic interphase modeled by it (Hashin, 1990, 1991a,b). Benveniste and Miloh has considered a thin curved isotropic layer of constant thickness between two elastic isotropic media in a two-dimensional plane strain problem. They show seven different conditions of contact interface: vacuous contact type interface; spring type interface; ideal contact interface; membrane type interface; inextensible membrane type interface; inextensible shell type interface and rigid contact type interface; rigid contact type interface (see, Benveniste and Miloh, 2001).

The novelty of this contribution is based on overcoming the challenge of simulating mechanical behavior of composites with spring imperfect adherence between the matrix and the reinforcements, i.e. the discontinuity of displacements is linearly proportional to the traction vector. It is assumed that the imperfect parameters are inversely proportional to the radius of the fibers. The model presented include as limit cases: vacuous contact type interface and ideal contact interface. In this sense, the formulation of the local problems for two phase linear elastic composites with spring imperfect contact conditions is given and the solution of each local problems is found using the semi-analytic method where the differential equations derived from the local problems by asymptotic homogenization method (AHM) are solved using the finite element method with quadrilateral of eight nodes, implemented via Fortran code. Besides, the expressions for the effective elastic coefficients of a fiber reinforced composite with circular cylindrical shape periodically distributed in the matrix under linear spring imperfect contact conditions are obtained via AHM.

* Corresponding author.
E-mail address: jaotero@icimaf.cu (J.A. Otero).

0020-7683/$ - see front matter © 2012 Elsevier Ltd. All rights reserved.
http://dx.doi.org/10.1016/j.ijsolstr.2012.11.001

2. Statement of the problem for heterogeneous media

Consider an heterogeneous media occupying a volume $\Omega \in \Re^3$ with boundary $\partial\Omega = \partial_1\Omega \cup \partial_2\Omega$ and consisting of two-phase uniaxial reinforced material, where fibers and matrix have transversely isotropic elastic properties; the axis of transverse symmetry coincides with the fiber direction, which is taken as the Ox_3 axis. The fibers with circular cross section are periodically distributed along the Ox_1 and Ox_2 axis directions (see, Fig. 1). The governing equations for the static elasticity heterogeneous problems are

$$\frac{\partial \sigma_{ij}}{\partial x_j} = 0, \quad \text{in } \Omega, \tag{2.1}$$

$$\begin{aligned} &u_i = 0, \quad \text{on } \partial_1\Omega, \\ &\sigma_{ij} n_j = 0, \quad \text{on } \partial_2\Omega, \end{aligned} \tag{2.2}$$

where $i,j = 1,2,3$ and $\sigma_{ij},\ u_i,\ n_j$ are the stress tensor components, the displacement vector components and normal unit vector components on $\partial_2\Omega$, respectively. The constitutive equations and the strain tensor components ε_{kl} are given by

$$\sigma_{ij} = C_{ijkl}(\mathbf{y})\varepsilon_{kl}, \tag{2.3}$$

$$\varepsilon_{kl} = \frac{1}{2}\left(\frac{\partial u_k}{\partial x_l} + \frac{\partial u_l}{\partial x_k}\right). \tag{2.4}$$

Here the elastic coefficients $C_{ijkl}(\mathbf{y})$ $(i,j,k,l = 1,2,3)$ are Y-periodic functions and $\mathbf{y} = \mathbf{x}/\alpha$ is called the local variable that are defined on the unit cell. α is a small parameter, which expresses the ratio between the periodic cell length and the characteristic length of the composite. The periodic unit cell S is taken as a regular square in the y_1y_2-plane so that $S = S_1 \cup S_2$ with $S_1 \cap S_2 = \emptyset$, where the domain S_2 is occupied by the matrix and its complement S_1 (fiber) is considered by a circle of radius R and center at the origin O (Fig. 1). The common interface between the fiber and the matrix is denoted by Γ. The fiber and matrix associated quantities are also referred below by means of super-indices in brackets (1) and (2), respectively.

The usually adopted ideal contact conditions consists in demanding the continuity of displacements and traction across the interface between the two solids. Considerer that the composite exhibits imperfect contact at the interface between the fiber and matrix, that is, the discontinuity of displacements is linearly proportional to the traction vector. This is called a "spring type" interface (Hashin, 1990). Using the vector notation, the elastic imperfect condition can be expressed as

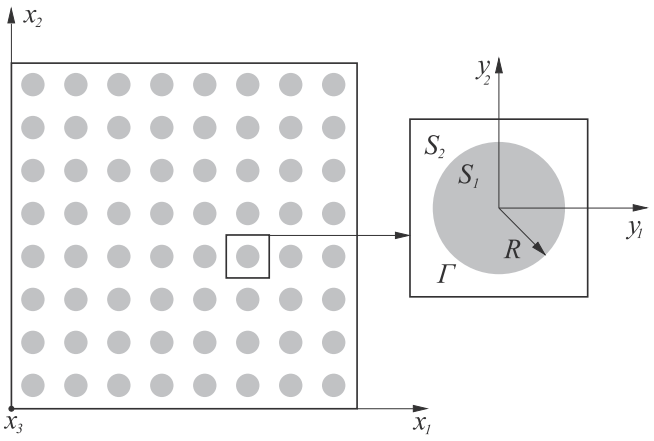

Fig. 1. The cross-section of a periodic composite array of circular fibers.

$$\mathbf{T}^{(1)} + \mathbf{T}^{(2)} = 0, \quad \mathbf{T}^{(\Upsilon)} = (-1)^{(\Upsilon+1)}\mathbf{K}\|\mathbf{u}\|, \quad \text{on } \Gamma, \tag{2.5}$$

where $\Upsilon = 1,2$ and $\|\bullet\|$ is the jump in the quantity at the common interface between the fiber and matrix. The elastic displacement vector $\mathbf{u}$, the traction vector $\mathbf{T}$ and spring stiffness matrix $\mathbf{K}$ are given by

$$\mathbf{u} = \begin{bmatrix} u_n \\ u_t \\ u_a \end{bmatrix}, \quad \mathbf{T} = \begin{bmatrix} T_n \\ T_t \\ T_a \end{bmatrix}, \quad \mathbf{K} = \begin{bmatrix} K_n & 0 & 0 \\ 0 & K_t & 0 \\ 0 & 0 & K_a \end{bmatrix}, \tag{2.6}$$

where $u_n,\ u_t$ and u_a are normal, tangential and axial components of displacement vector $\mathbf{u}$, respectively; $T_n,\ T_t$ and T_a are normal, tangential and axial components of traction vector $\mathbf{T}$ $(T_i = \sigma_{ij}n_j)$, respectively; $\mathbf{n}$ is the outward unit normal vector on Γ; K_n, K_t and K_a are normal, tangential and axial sprint constant material parameters (imperfect parameters), which have the physical dimension [pascal/meter]. It is assumed that the imperfect parameters are: $K_n = \kappa_n C^{(2)}_{1313}/R$, $K_t = \kappa_t C^{(2)}_{1313}/R$ and $K_a = \kappa_a C^{(2)}_{1313}/R$. Here $\kappa_n,\ \kappa_t$ and κ_a are normal, tangential and axial dimensionless imperfect parameters, respectively. The normal and tangential components of the displacement and traction vectors found in the x_1x_2-plane, while the axial component of the displacement and traction vectors coincides with the fiber direction (Ox_3-axis). Perfect contact is revealed when the spring imperfect parameters approaches to infinity, while the debonding contact takes place as these imperfect parameters approach to zero.

3. Asymptotic homogenization method. Homogeneous problem, local problems and effective coefficients

The overall properties of the above periodic medium are sought using the well-known asymptotic homogenization method (Bakhvalov and Panasenko, 1989; Sanchez-Palencia, 1980; Pobedrya, 1984). Now it is assumed that the elastic displacement vector components are given by the following expansion

$$u_i = u_i^{(0)}(\mathbf{x}) + \alpha u_i^{(1)}(\mathbf{x},\mathbf{y}) + \alpha^2 u_i^{(2)}(\mathbf{x},\mathbf{y}) + \cdots. \tag{3.1}$$

Here $i = 1,2,3$. Substituting (3.1) into (2.3) and (2.4) we obtain

$$\sigma_{ij} = \sigma_{ij}^{(0)}(\mathbf{x},\mathbf{y}) + \alpha\sigma_{ij}^{(1)}(\mathbf{x},\mathbf{y}) + \cdots, \tag{3.2}$$

$$\varepsilon_{ij} = \varepsilon_{ij}^{(0)}(\mathbf{x},\mathbf{y}) + \alpha\varepsilon_{ij}^{(1)}(\mathbf{x},\mathbf{y}) + \cdots, \tag{3.3}$$

where

$$\sigma_{ij}^{(0)}(\mathbf{x},\mathbf{y}) = C_{ijkl}(\mathbf{y})\frac{\partial u_k^{(0)}(\mathbf{x})}{\partial x_l} + C_{ijkl}(\mathbf{y})\frac{\partial u_k^{(1)}(\mathbf{x},\mathbf{y})}{\partial y_l}, \tag{3.4}$$

$$\sigma_{ij}^{(1)}(\mathbf{x},\mathbf{y}) = C_{ijkl}(\mathbf{y})\frac{\partial u_k^{(1)}(\mathbf{x},\mathbf{y})}{\partial x_l} + C_{ijkl}(\mathbf{y})\frac{\partial u_k^{(2)}(\mathbf{x},\mathbf{y})}{\partial y_l}, \tag{3.5}$$

$$\begin{aligned} \varepsilon_{ij}^{(0)}(\mathbf{x},\mathbf{y}) = &\frac{1}{2}\left(\frac{\partial u_i^{(0)}(\mathbf{x})}{\partial x_j} + \frac{\partial u_j^{(0)}(\mathbf{x})}{\partial x_i}\right) \\ &+ \frac{1}{2}\left(\frac{\partial u_i^{(1)}(\mathbf{x},\mathbf{y})}{\partial y_j} + \frac{\partial u_j^{(1)}(\mathbf{x},\mathbf{y})}{\partial y_i}\right), \end{aligned} \tag{3.6}$$

$$\begin{aligned} \varepsilon_{ij}^{(1)}(\mathbf{x},\mathbf{y}) = &\frac{1}{2}\left(\frac{\partial u_i^{(1)}(\mathbf{x},\mathbf{y})}{\partial x_j} + \frac{\partial u_j^{(1)}(\mathbf{x},\mathbf{y})}{\partial x_i}\right) \\ &+ \frac{1}{2}\left(\frac{\partial u_i^{(2)}(\mathbf{x},\mathbf{y})}{\partial y_j} + \frac{\partial u_j^{(2)}(\mathbf{x},\mathbf{y})}{\partial y_i}\right), \end{aligned} \tag{3.7}$$

Using (3.1) and (3.2) in (2.1) and rearranging the terms of equal exponent of α we have for α^{-1} and α^0

$$\frac{\partial \sigma_{ij}^{(0)}(\mathbf{x},\mathbf{y})}{\partial y_j} = 0, \tag{3.8}$$

$$\frac{\partial \sigma_{ij}^{(0)}(\mathbf{x},\mathbf{y})}{\partial x_j} + \frac{\partial \sigma_{ij}^{(1)}(\mathbf{x},\mathbf{y})}{\partial y_j} = 0. \tag{3.9}$$

Substituting (3.4) in (3.8) we obtain

$$\frac{\partial}{\partial y_j}\left(C_{ijkl}(\mathbf{y})\frac{\partial u_k^{(1)}(\mathbf{x},\mathbf{y})}{\partial y_l}\right) = -\frac{\partial u_k^{(0)}(\mathbf{x})}{\partial x_l}\frac{\partial C_{ijkl}(\mathbf{y})}{\partial y_j}. \tag{3.10}$$

The function $u_k^{(1)}(\mathbf{x},\mathbf{y})$ is given according to

$$u_k^{(1)}(\mathbf{x},\mathbf{y}) = {}_{pq}N_k(\mathbf{y})\frac{\partial u_p^{(0)}(\mathbf{x})}{\partial x_q}, \tag{3.11}$$

where ${}_{pq}N_k(\mathbf{y})$ $(k,p,q=1,2,3)$ are Y-periodic local displacement vector components.

The pq local problems on the periodic cell may arise replacing (3.11) into (3.10) and the following expression is obtained

$$\frac{\partial\, {}_{pq}\tau_{ij}(\mathbf{y})}{\partial y_j} = -\frac{\partial C_{ijpq}(\mathbf{y})}{\partial y_j}, \tag{3.12}$$

where the Y-periodic local stress tensor components are

$${}_{pq}\tau_{ij}(\mathbf{y}) = C_{ijkl}(\mathbf{y})\frac{\partial_{pq}N_k(\mathbf{y})}{\partial y_l}. \tag{3.13}$$

The imperfect contact conditions given in (2.5) are transformed by

$${}_{pq}\mathbf{T}^{(1)} + {}_{pq}\mathbf{T}^{(2)} = 0, \quad {}_{pq}\mathbf{T}^{(\Upsilon)} = (-1)^{(\Upsilon+1)}\mathbf{K}\|_{pq}\mathbf{N}\|, \quad \text{on } \Gamma. \tag{3.14}$$

The local elastic displacement vector ${}_{pq}\mathbf{N}$ and the local traction vector ${}_{pq}\mathbf{T}$ are

$${}_{pq}\mathbf{N} = \begin{bmatrix} {}_{pq}N_n \\ {}_{pq}N_t \\ {}_{pq}N_a \end{bmatrix}, \quad {}_{pq}\mathbf{T} = \begin{bmatrix} {}_{pq}T_n \\ {}_{pq}T_t \\ {}_{pq}T_a \end{bmatrix}, \tag{3.15}$$

and ${}_{pq}N_n$, ${}_{pq}N_t$, ${}_{pq}N_a$ are normal, tangential and axial components of local displacement vector ${}_{pq}\mathbf{N}$, respectively; ${}_{pq}T_n$, ${}_{pq}T_t$, ${}_{pq}T_a$ are normal, tangential and axial components of local traction vector ${}_{pq}\mathbf{T}$ $({}_{pq}T_i = {}_{pq}\tau_{ij}(\mathbf{y})\,n_j + C_{ijpq}(\mathbf{y})\,n_j)$, respectively.

Now, substituting (3.11) into (3.4) and (3.6) we obtain

$$\sigma_{ij}^{(0)}(\mathbf{x},\mathbf{y}) = \left(C_{ijpq}(\mathbf{y}) + {}_{pq}\tau_{ij}(\mathbf{y})\right)\frac{\partial u_p^{(0)}(\mathbf{x})}{\partial x_q}, \tag{3.16}$$

$$\varepsilon_{ij}^{(0)}(\mathbf{x},\mathbf{y}) = \frac{1}{2}\left(\frac{\partial u_i^{(0)}(\mathbf{x})}{\partial x_j} + \frac{\partial u_j^{(0)}(\mathbf{x})}{\partial x_i}\right) + \frac{1}{2}\left(\frac{\partial_{pq}N_i(\mathbf{y})}{\partial y_j} + \frac{\partial_{pq}N_j(\mathbf{y})}{\partial y_i}\right)\frac{\partial u_p^{(0)}(\mathbf{x})}{\partial x_q}. \tag{3.17}$$

Let us define the average over the periodic cell

$$< \bullet >= \frac{1}{|Y|}\int_Y (\bullet)dy, \tag{3.18}$$

where $|Y|$ is the volume of the cell. Taking the average of expression (3.9) and using the periodicity of $\sigma_{ij}^{(1)}$, the homogeneous static problem is obtained as follows

$$\frac{\partial \overline{\sigma}_{ij}^{(0)}(\mathbf{x})}{\partial x_j} = 0, \tag{3.19}$$

where the homogeneous constitutive equations are

$$\overline{\sigma}_{ij}^{(0)}(\mathbf{x}) = \sigma_{ij}^{(0)}(\mathbf{x},\mathbf{y}) = C_{ijpq}^{*}\frac{\partial u_p^{(0)}(\mathbf{x})}{\partial x_q}, \tag{3.20}$$

and

$$C_{ijpq}^{*} = C_{ijpq}(\mathbf{y}) + {}_{pq}\tau_{ij}(\mathbf{y}), \tag{3.21}$$

are the effective elastic coefficients. Applying the average operator on the expression (3.17) and using the periodicity of ${}_{pq}\mathbf{N}(\mathbf{y})$, the homogeneous strain tensor is

$$\overline{\varepsilon}_{ij}^{(0)}(\mathbf{x}) = \left\langle \varepsilon_{ij}^{(0)}(\mathbf{x},\mathbf{y}) \right\rangle = \frac{1}{2}\left(\frac{\partial u_i^{(0)}(\mathbf{x})}{\partial x_j} + \frac{\partial u_j^{(0)}(\mathbf{x})}{\partial x_i}\right). \tag{3.22}$$

The boundary conditions given in (2.2) are transformed by

$$\begin{aligned} &u_i^{(0)}(\mathbf{x}) = 0, \quad \text{on } \partial_1\Omega, \\ &\overline{\sigma}_{ij}^{(0)}(\mathbf{x})\,n_j = 0, \quad \text{on } \partial_2\Omega. \end{aligned} \tag{3.23}$$

The main problem to obtain effective coefficients is to find the periodic solutions of six ${}_{pq}L$ local problems on S in terms of the local variable $\mathbf{y}$, where $p,q=1,2,3$. Each local problem decouples into independent sets of equations, i.e. plane-strain and antiplane-strain systems. In the following Table 1, the correspondence between the effective properties and the local problems is shown.

The local problems for circular fibrous elastic composite with perfect contact at the interface and periodic conditions over the unit cell are analytically solved in Rodriguez-Ramos et al. (2001). However, analytic solutions for the local problems of composites with other type of reinforcement geometric shape are difficult to find (for instance, square fibers). In this case, suitable numerical methods are the necessary tools to be applied. This numerical procedure is simplified when some symmetry elements occur in the geometry of the unit cell and/or in the constituent properties, because a local problem for the entire unit cell may be reduced to boundary value problem for only a part of the cell.

In our problem, the elastic coefficients $C_{ijkl}(\mathbf{y}) \equiv C_{ijkl}(y_1,y_2)$ are even functions with respect to y_1 and y_2, then satisfy the following conditions (see, Bakhvalov and Panasenko, 1989)

$${}_{pq}N_i|_{y_h=0,1/2} = 0, \quad \text{for } \delta_{hi}+\delta_{hp}+\delta_{hq} \text{ odd}, \tag{3.24}$$

$${}_{pq}\tau_{hi}|_{y_h=0,1/2} = 0, \quad \text{for } \delta_{hi}+\delta_{hp}+\delta_{hq}+1 \text{ odd}, \tag{3.25}$$

where $h=1,2$; $i,p,q=1,2,3$ and

$$\delta_{hi} = \begin{cases} 1 & \text{for } h=i, \\ 0 & \text{for } h\neq i. \end{cases} \tag{3.26}$$

Using the condition (3.24) and (3.25) the ${}_{pq}L$ local problems over the periodic unit cell can be transformed to boundary value problems over 1/4 unit cell. Passing now the ${}_{pq}L$ local problems to the new variable ${}_{pq}M_k$ as follows

$${}_{pq}N_k = {}_{pq}M_k - y_p\,\delta_{lq}, \tag{3.27}$$

where $p,q,l=1,2,3$. Eq. (3.13) can be written as

$${}_{pq}\tau_{ij}(\mathbf{y}) = {}_{pq}\sigma_{ij}(\mathbf{y}) - C_{ijpq}(\mathbf{y}). \tag{3.28}$$

Here we have denoted

Table 1
Effective properties related to the local problems.

${}_{11}L$	${}_{22}L$	${}_{33}L$	${}_{23}L$	${}_{13}L$	${}_{12}L$
C_{1111}^{*}	C_{1122}^{*}	C_{1133}^{*}	0	0	0
C_{2211}^{*}	C_{2222}^{*}	C_{2233}^{*}	0	0	0
C_{3311}^{*}	C_{3322}^{*}	C_{3333}^{*}	0	0	0
0	0	0	C_{2323}^{*}	0	0
0	0	0	0	C_{1313}^{*}	0
0	0	0	0	0	C_{1212}^{*}

$$ {}_{pq}\sigma_{ij}(\mathbf{y}) = C_{ijkl}(\mathbf{y})\frac{\partial_{pq}M_k(\mathbf{y})}{\partial y_l}, \tag{3.29} $$

and Eqs. (3.12) and (3.21) are transformed by

$$ \frac{\partial_{pq}\sigma_{ij}(\mathbf{y})}{\partial y_j} = 0, \tag{3.30} $$

$$ C^*_{ijpq} = 4\langle {}_{pq}\sigma_{ij}(\mathbf{y})\rangle. \tag{3.31} $$

Finally, the ${}_{pq}L$ local problems can be written in the following form using the abbreviate notation for the elastic coefficients C_{ijkl}.

3.1. The antiplane problem ${}_{\lambda 3}L$

The local antiplane problem over 1/4 of the cell is expressed by

$$ \frac{\partial_{\lambda 3}\sigma^{(\Upsilon)}_{13}}{\partial y_1} + \frac{\partial_{\lambda 3}\sigma^{(\Upsilon)}_{23}}{\partial y_2} = 0, \tag{3.32} $$

where

$$ {}_{\lambda 3}\sigma^{(\Upsilon)}_{13} = C^{(\Upsilon)}_{55}\frac{\partial_{\lambda 3}M^{(\Upsilon)}_3}{\partial y_1}, \tag{3.33} $$

$$ {}_{\lambda 3}\sigma^{(\Upsilon)}_{23} = C^{(\Upsilon)}_{44}\frac{\partial_{\lambda 3}M^{(\Upsilon)}_3}{\partial y_2}, \tag{3.34} $$

Greek, upper and lower, indices runs from 1 to 2.

The imperfect contact conditions for the ${}_{\lambda 3}L$ local problems are written in the following form

$$ {}_{\lambda 3}T^{(1)}_3 = -{}_{\lambda 3}T^{(2)}_3 = \frac{\kappa_a C^{(2)}_{55}}{R}\left({}_{\lambda 3}M^{(1)}_3 - {}_{\lambda 3}M^{(2)}_3\right) \quad \text{on } \Gamma, \tag{3.35} $$

where ${}_{\lambda 3}T^{(\Upsilon)}_3$ is the component of traction force in the y_3-direction given by ${}_{\lambda 3}T_3 = {}_{\lambda 3}\sigma_{j3}n_j$, ${}_{\lambda 3}M^{(\Upsilon)}_3$ is the component in the y_3-direction of displacement vector.

The boundary conditions are given as,

$$ {}_{\lambda 3}M^{(\Upsilon)}_3 = 0, \quad \text{for } y_\lambda = 0, \quad y_\beta \in S_\Upsilon, \tag{3.36} $$

$$ {}_{\lambda 3}M^{(\Upsilon)}_3 = \frac{1}{2}, \quad \text{for } y_\lambda = \frac{1}{2}, \quad y_\beta \in S_\Upsilon, \tag{3.37} $$

$$ {}_{\lambda 3}\sigma^{(\Upsilon)}_{\beta 3} = 0, \quad \text{for } y_\lambda \in S_\Upsilon, \quad y_\beta = 0, \tag{3.38} $$

$$ {}_{\lambda 3}\sigma^{(\Upsilon)}_{\beta 3} = 0, \quad \text{for } y_\lambda \in S_\Upsilon, \quad y_\beta = \frac{1}{2}, \tag{3.39} $$

where $\lambda = 1$ and $\beta = 2$ for the ${}_{13}L$ local problem, whilst $\lambda = 2$ and $\beta = 1$ for the ${}_{23}L$ local problem.

The effective coefficients can be calculated using the following expressions (see, Eq. (3.31))

$$ C^*_{55} = 4\left\langle C_{55}\frac{\partial_{13}M_3}{\partial y_1}\right\rangle, \quad C^*_{44} = 4\left\langle C_{44}\frac{\partial_{23}M_3}{\partial y_2}\right\rangle. \tag{3.40} $$

3.2. The plane problem ${}_{\beta\beta}L$

Again for the sake of clarity, in this section let ${}_{\beta\beta}\mathbf{M}^{(\Upsilon)} \equiv ({}_{\beta\beta}M^{(\Upsilon)}_1,\ {}_{\beta\beta}M^{(\Upsilon)}_2)$ and the $\beta\beta$ pre-subscripts are 11, 22, then the statement of the problems is

$$ \frac{\partial_{\beta\beta}\sigma^{(\Upsilon)}{}_{11}}{\partial y_1} + \frac{\partial_{\beta\beta}\sigma^{(\Upsilon)}_{12}}{\partial y_2} = 0, \tag{3.41} $$

$$ \frac{\partial_{\beta\beta}\sigma^{(\Upsilon)}_{21}}{\partial y_1} + \frac{\partial_{\beta\beta}\sigma^{(\Upsilon)}_{22}}{\partial y_2} = 0, \tag{3.42} $$

where

$$ {}_{\beta\beta}\sigma^{(\Upsilon)}{}_{11} = C^{(\Upsilon)}{}_{11}\frac{\partial_{\beta\beta}M^{(\Upsilon)}_1}{\partial y_1} + C^{(\Upsilon)}_{12}\frac{\partial_{\beta\beta}M^{(\Upsilon)}_2}{\partial y_2}, \tag{3.43} $$

$$ {}_{\beta\beta}\sigma^{(\Upsilon)}_{22} = C^{(\Upsilon)}_{12}\frac{\partial_{\beta\beta}M^{(\Upsilon)}_1}{\partial y_1} + C^{(\Upsilon)}_{22}\frac{\partial_{\beta\beta}M^{(\Upsilon)}_2}{\partial y_2}, \tag{3.44} $$

$$ {}_{\beta\beta}\sigma^{(\Upsilon)}_{12} = {}_{\beta\beta}\sigma^{(\Upsilon)}_{21} = C^{(\Upsilon)}_{66}\left(\frac{\partial_{\beta\beta}M^{(\Upsilon)}_1}{\partial y_2} + \frac{\partial_{\beta\beta}M^{(\Upsilon)}_2}{\partial y_1}\right). \tag{3.45} $$

The imperfect contact conditions for the ${}_{\beta\beta}L$ local problems are written in the following form

$$ {}_{\beta\beta}T^{(1)}_t = -{}_{\beta\beta}T^{(2)}_t = \frac{\kappa_t C^{(2)}_{55}}{R}\left({}_{\beta\beta}M^{(1)}_t - {}_{\beta\beta}M^{(2)}_t\right), \tag{3.46} $$

$$ {}_{\beta\beta}T^{(1)}_n = -{}_{\beta\beta}T^{(2)}_n = \frac{\kappa_n C^{(2)}_{55}}{R}\left({}_{\beta\beta}M^{(1)}_n - {}_{\beta\beta}M^{(2)}_n\right), \tag{3.47} $$

where ${}_{\beta\beta}T^{(\Upsilon)}_t$ (${}_{\beta\beta}T^{(\Upsilon)}_n$) is the tangential (normal) component of traction force ${}_{\beta\beta}T_i = {}_{\beta\beta}\sigma_{ij}n_j$; ${}_{\beta\beta}M^{(\Upsilon)}_t$ (${}_{\beta\beta}M^{(\Upsilon)}_n$) is the tangential (normal) component of displacement vector ${}_{\beta\beta}\mathbf{M}^{(\Upsilon)}$.

The boundary conditions associated to this problem are given as,

$$ {}_{\beta\beta}M^{(\Upsilon)}_1 = 0, \quad {}_{\beta\beta}\sigma^{(\Upsilon)}_{12} = 0, \quad \text{for } y_1 = 0,\ y_2 \in S_\Upsilon, \tag{3.48} $$

$$ {}_{\beta\beta}M^{(\Upsilon)}_1 = \frac{1}{2}\alpha_1, \quad {}_{\beta\beta}\sigma^{(\Upsilon)}_{12} = 0, \quad \text{for } y_1 = \frac{1}{2},\ y_2 \in S_\Upsilon, \tag{3.49} $$

$$ {}_{\beta\beta}M^{(\Upsilon)}_2 = 0, \quad {}_{\beta\beta}\sigma^{(\Upsilon)}_{21} = 0, \quad \text{for } y_1 \in S_\Upsilon,\ y_2 = 0, \tag{3.50} $$

$$ {}_{\beta\beta}M^{(\Upsilon)}_2 = \frac{1}{2}\alpha_2, \quad {}_{\beta\beta}\sigma^{(\Upsilon)}_{21} = 0, \quad \text{for } y_1 \in S_\Upsilon,\ y_2 = \frac{1}{2}, \tag{3.51} $$

where $\alpha_1 = 1$ and $\alpha_2 = 0$ for the ${}_{11}L$ local problem whereas $\alpha_1 = 0$ and $\alpha_2 = 1$ for the ${}_{22}L$ local problem. Notice that the ${}_{33}L$ local problem has not been mentioned since, as it was previously stated, it can be connected with the ${}_{11}L$ and ${}_{22}L$ problems by the formula (3.2), (Rodriguez-Ramos et al., 2001).

The formulae for computing the effective coefficients are listed as follows (see, Eq. (3.31) and Rodriguez-Ramos et al., 2001)

$$ \begin{aligned}
&C^*_{11} = 4\left\langle C_{11}\frac{\partial_{11}M_1}{\partial y_1} + C_{12}\frac{\partial_{11}M_2}{\partial y_2}\right\rangle, \quad C^*_{21} = 4\left\langle C_{12}\frac{\partial_{11}M_1}{\partial y_1} + C_{11}\frac{\partial_{11}M_2}{\partial y_2}\right\rangle,\\
&C^*_{31} = 4\left\langle C_{13}\left(\frac{\partial_{11}M_1}{\partial y_1} + \frac{\partial_{11}M_2}{\partial y_2}\right)\right\rangle, \quad C^*_{12} = 4\left\langle C_{11}\frac{\partial_{22}M_1}{\partial y_1} + C_{12}\frac{\partial_{22}M_2}{\partial y_2}\right\rangle,\\
&C^*_{22} = 4\left\langle C_{12}\frac{\partial_{22}M_1}{\partial y_1} + C_{11}\frac{\partial_{22}M_2}{\partial y_2}\right\rangle, C^*_{32} = 4\left\langle C_{13}\left(\frac{\partial_{22}M_1}{\partial y_1} + \frac{\partial_{22}M_2}{\partial y_2}\right)\right\rangle,\\
&C^*_{13} = 4\langle C_{13}\rangle - \frac{4\|C_{13}\|}{\|C_{11}+C_{12}\|}\langle C_{11}+C_{12}\rangle + \frac{\|C_{13}\|}{\|C_{11}+C_{12}\|}(C^*_{11}+C^*_{12}),\\
&C^*_{23} = 4\langle C_{13}\rangle - \frac{4\|C_{13}\|}{\|C_{11}+C_{12}\|}\langle C_{11}+C_{12}\rangle + \frac{\|C_{13}\|}{\|C_{11}+C_{12}\|}(C^*_{21}+C^*_{22}),\\
&C^*_{33} = 4\langle C_{33}\rangle - \frac{8\|C_{13}\|}{\|C_{11}+C_{12}\|}\langle C_{13}\rangle + \frac{\|C_{13}\|}{\|C_{11}+C_{12}\|}(C^*_{31}+C^*_{32}).
\end{aligned} \tag{3.52} $$

The double bar notation denotes the jump of the function $f(\mathbf{y})$ across the interface, i.e.,

$$ \|f(\mathbf{y})\| = f^{(1)}(\mathbf{y}) - f^{(2)}(\mathbf{y}). \tag{3.53} $$

3.3. The plane problem ${}_{12}L$

Again, in this section let ${}_{12}\mathbf{M}^{(\Upsilon)} \equiv ({}_{12}M^{(\Upsilon)}_1,\ {}_{12}M^{(\Upsilon)}_2)$, then the statement of the problem is

$$\frac{\partial_{12}\sigma_{11}^{(\Upsilon)}}{\partial y_1}+\frac{\partial_{12}\sigma_{12}^{(\Upsilon)}}{\partial y_2}=0, \tag{3.54}$$

$$\frac{\partial_{12}\sigma_{21}^{(\Upsilon)}}{\partial y_1}+\frac{\partial_{12}\sigma_{22}^{(\Upsilon)}}{\partial y_2}=0, \tag{3.55}$$

where

$${}_{12}\sigma_{11}^{(\Upsilon)}=C_{11}^{(\Upsilon)}\frac{\partial_{12}M_1^{(\Upsilon)}}{\partial y_1}+C_{12}^{(\Upsilon)}\frac{\partial_{12}M_2^{(\Upsilon)}}{\partial y_2}, \tag{3.56}$$

$${}_{12}\sigma_{22}^{(\Upsilon)}=C_{12}^{(\Upsilon)}\frac{\partial_{12}M_1^{(\Upsilon)}}{\partial y_1}+C_{22}^{(\Upsilon)}\frac{\partial_{12}M_2^{(\Upsilon)}}{\partial y_2}, \tag{3.57}$$

$${}_{12}\sigma_{12}^{(\Upsilon)}={}_{12}\sigma_{21}^{(\Upsilon)}=C_{66}^{(\Upsilon)}\left(\frac{\partial_{12}M_1^{(\Upsilon)}}{\partial y_2}+\frac{\partial_{12}M_2^{(\Upsilon)}}{\partial y_1}\right). \tag{3.58}$$

The imperfect contact conditions for the ${}_{12}L$ local problem are written in the following form

$${}_{12}T_t^{(1)}=-{}_{12}T_t^{(2)}=\frac{\kappa_t C_{55}^{(2)}}{R}\left({}_{12}M_t^{(1)}-{}_{12}M_t^{(2)}\right), \tag{3.59}$$

$${}_{12}T_n^{(1)}=-{}_{12}T_n^{(2)}=\frac{\kappa_n C_{55}^{(2)}}{R}\left({}_{12}M_n^{(1)}-{}_{12}M_n^{(2)}\right), \tag{3.60}$$

where ${}_{12}T_t^{(\Upsilon)}$ (${}_{12}T_n^{(\Upsilon)}$) is the tangential (normal) component of traction force ${}_{12}T_i={}_{12}\sigma_{ij}n_j$ and ${}_{12}M_t^{(\Upsilon)}$ (${}_{12}M_n^{(\Upsilon)}$) is the tangential (normal) component of displacement vector ${}_{12}\mathbf{M}^{(\Upsilon)}$.

The boundary conditions are given as,

$${}_{12}M_1^{(\Upsilon)}=0,\quad {}_{12}\sigma_{21}^{(\Upsilon)}=0,\quad \text{for } y_1\in S_\Upsilon,\ y_2=0, \tag{3.61}$$

$${}_{12}M_1^{(\Upsilon)}=\frac{1}{2}\alpha_3^{(\Upsilon)},\quad {}_{12}\sigma_{21}^{(\Upsilon)}=0,\quad \text{for } y_1\in S_\Upsilon,\ y_2=\frac{1}{2}, \tag{3.62}$$

$${}_{12}M_2^{(\Upsilon)}=0,\quad {}_{12}\sigma_{12}^{(\Upsilon)}=0,\quad \text{for } y_1=0,\ y_2\in S_\Upsilon, \tag{3.63}$$

$${}_{12}M_2^{(\Upsilon)}=\frac{1}{2}\alpha_4^{(\Upsilon)},\quad {}_{12}\sigma_{12}^{(\Upsilon)}=0,\quad \text{for } y_1=\frac{1}{2},\ y_2\in S_\Upsilon, \tag{3.64}$$

where α_3 and α_4 are constants which satisfy the relation $\alpha_3+\alpha_4=1$.

The effective coefficient can be calculated using the following expression (see, Eq. (3.31))

$$C_{66}^{*}=4\left\langle C_{66}\left(\frac{\partial_{12}M_1}{\partial y_2}+\frac{\partial_{12}M_2}{\partial y_1}\right)\right\rangle. \tag{3.65}$$

4. Implementation of finite element method for the local problems

Sometimes, the systems of equations that described the aforementioned local problems can not be solved analytically. Therefore, exact solutions only can be found for certain geometry of the fibers, for instance, circular fibers. For some other cases, it is very difficult to obtain exact solutions. One alternative method for solving the local problems is an approximate method, such as the formulation of the potential energy which require less conditions for the unknown functions. This is one of the reasons for using the principle of minimum potential energy combined with the finite element method in the present work. The potential energy of an elastic solid body is

$$\Pi=\frac{1}{2}\int_V\sigma^T\varepsilon\,dV-\int_V u^T f\,dV-\int_S u^T T\,dS-\sum_i u_i^T P_i. \tag{4.1}$$

This expression involves the following energies: the strain energy per unit volume in the body, the potential energy associated to body force (f), traction force (T) and point load force (P_i) respectively. In this work, $f=P_i=0$ and for sake of brevity only the finite element implementation of the antiplane local problem ${}_{13}L$ and the plane local problem ${}_{11}L$ will be shown. The remaining local problems are implemented in a similar form.

4.1 The antiplane problem ${}_{13}L$

The relations (3.33) and (3.34) for $\alpha=1$ can be written in matrix form as

$${}_{13}\sigma=\mathbf{D}\,{}_{13}\varepsilon, \tag{4.2}$$

where

$${}_{13}\sigma=\left[\,{}_{13}\sigma_{13}\quad {}_{13}\sigma_{23}\,\right]^T, \tag{4.3}$$

$${}_{13}\varepsilon=\left[\,{}_{13}\varepsilon_{13}\quad {}_{13}\varepsilon_{23}\,\right]^T=\left[\frac{\partial\,{}_{13}M_3}{\partial y_1}\quad \frac{\partial\,{}_{13}M_3}{\partial y_2}\right]^T,\quad u={}_{13}M_3, \tag{4.4}$$

$$\mathbf{D}=\begin{bmatrix}C_{55} & 0\\ 0 & C_{55}\end{bmatrix}. \tag{4.5}$$

The two-dimensional region is divided into a finite number of quadrilateral elements (see, Fig. 2). The element consists of eight nodes, all of which are located on the element boundary. The displacements inside the element are now written using the shape function and the nodal values of the unknown displacement field. Therefore, we have

$${}_{13}M_3=\Psi\mathbf{q}, \tag{4.6}$$

here $\mathbf{q}=[q_{31}\ q_{32}\ q_{33}\ q_{34}\ q_{35}\ q_{36}\ q_{37}\ q_{38}]^T$ where q_{3i} are the displacement components in y_3-direction of a local node $i=1,\ldots,8$ and $\Psi=[\psi_1\ \psi_2\ \psi_3\ \psi_4\ \psi_5\ \psi_6\ \psi_7\ \psi_8]$, ψ_i are the shape functions of the element given in natural coordinates by Zienkiewicz and Taylor (2000)

$$\begin{aligned}
\psi_1&=-\frac{(1-\xi)(1-\eta)(1+\xi+\eta)}{4},\quad \psi_5=\frac{(1-\xi^2)(1-\eta)}{2},\\
\psi_2&=-\frac{(1+\xi)(1-\eta)(1-\xi+\eta)}{4},\quad \psi_6=\frac{(1+\xi)(1-\eta^2)}{2},\\
\psi_3&=-\frac{(1+\xi)(1+\eta)(1-\xi-\eta)}{4},\quad \psi_7=\frac{(1-\xi^2)(1+\eta)}{2},\\
\psi_4&=-\frac{(1-\xi)(1+\eta)(1+\xi-\eta)}{4},\quad \psi_8=\frac{(1-\xi)(1-\eta^2)}{2}.
\end{aligned} \tag{4.7}$$

The strain-displacement relation (4.4) in natural coordinates can be written in the form

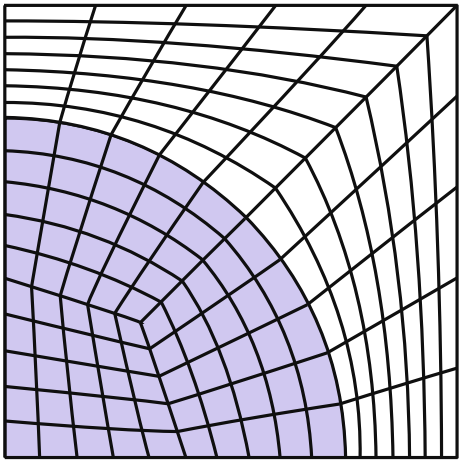

Fig. 2. Geometric mesh for 1/4 periodic cell.

$$\varepsilon = \begin{bmatrix} \frac{\partial\, {}_{13}M_3}{\partial y_1} \\ \frac{\partial\, {}_{13}M_3}{\partial y_2} \end{bmatrix} = \frac{1}{\det(\mathbf{J})} \begin{bmatrix} J_{22} & -J_{12} \\ -J_{21} & J_{11} \end{bmatrix} \begin{bmatrix} \frac{\partial\, {}_{13}M_3}{\partial \xi} \\ \frac{\partial\, {}_{13}M_3}{\partial \eta} \end{bmatrix}, \tag{4.8}$$

where $\mathbf{J}$ is the Jacobian of the transformation,

$$\mathbf{J} = \begin{bmatrix} J_{11} & J_{12} \\ J_{21} & J_{22} \end{bmatrix} = \begin{bmatrix} \frac{\partial x}{\partial \xi} & \frac{\partial y}{\partial \xi} \\ \frac{\partial x}{\partial \eta} & \frac{\partial y}{\partial \eta} \end{bmatrix}. \tag{4.9}$$

Using (4.6) and (4.8) the strain can be written in matrix form as

$$\varepsilon = \mathbf{B}\mathbf{q}, \tag{4.10}$$

where $\mathbf{B}$ is a 2×8 element strain-displacement matrix

$$\mathbf{B} = \frac{1}{\det(\mathbf{J})} \begin{bmatrix} J_{22} & -J_{12} \\ -J_{12} & J_{11} \end{bmatrix} \begin{bmatrix} \frac{\partial \psi_1}{\partial \xi} & \frac{\partial \psi_2}{\partial \xi} & \frac{\partial \psi_3}{\partial \xi} & \frac{\partial \psi_4}{\partial \xi} & \frac{\partial \psi_5}{\partial \xi} & \frac{\partial \psi_6}{\partial \xi} & \frac{\partial \psi_7}{\partial \xi} & \frac{\partial \psi_8}{\partial \xi} \\ \frac{\partial \psi_1}{\partial \eta} & \frac{\partial \psi_2}{\partial \eta} & \frac{\partial \psi_3}{\partial \eta} & \frac{\partial \psi_4}{\partial \eta} & \frac{\partial \psi_5}{\partial \eta} & \frac{\partial \psi_6}{\partial \eta} & \frac{\partial \psi_7}{\partial \eta} & \frac{\partial \psi_8}{\partial \eta} \end{bmatrix}. \tag{4.11}$$

Now, the stress values need to be calculated for each element. Using the stress-strain relations (4.2) and the element strain-displacement matrix (4.10) we have

$$\sigma = \mathbf{D}\mathbf{B}\mathbf{q}. \tag{4.12}$$

4.1.1. Element stiffness matrix

The strain energy associated with one plane element is obtained by

$$\Pi_S^e = t_e \int_e \frac{1}{2} \sigma^T \varepsilon \, dA, \tag{4.13}$$

taking the element thickness t_e as constant over the element and replacing (4.10), (4.12) into (4.13) we obtain the strain energy in the form

$$\Pi_S^e = \frac{1}{2} \mathbf{q}^T \mathbf{K}_S^e \mathbf{q}, \tag{4.14}$$

where $\mathbf{K}_S^e$ is the element stiffness matrix

$$\mathbf{K}_s^e = t_e \int_{-1}^{1} \int_{-1}^{1} \mathbf{B}^T \mathbf{D} \mathbf{B} \det(\mathbf{J}) \, d\xi \, d\eta. \tag{4.15}$$

Considering the contribution of all the elements to strain potential energy we obtain

$$\Pi_S = \sum_e \Pi_S^e = \sum_e \frac{1}{2} \mathbf{q}^T \mathbf{K}_S^e \mathbf{q} = \frac{1}{2} \mathbf{Q}^T \mathbf{K}_S \mathbf{Q}, \tag{4.16}$$

where $\mathbf{K}_S$ ($\mathbf{Q}$) is the global stiffness matrix (global displacement vector).

4.1.2. Effective coefficient

The substitution of $\partial\, {}_{13}M_3/\partial y_1$, (4.6) and (4.8) into (3.40a) gives the contribution by the element (e) in the effective coefficient as

$${}^eC_{55}^* = 4 \int_{-1}^{1} \int_{-1}^{1} \overline{\mathbf{D}}\, \overline{\mathbf{B}} \mathbf{q} \det(\mathbf{J}) \, d\xi \, d\eta, \tag{4.17}$$

where $\overline{\mathbf{D}} = {}^eC_{55}$ and

$$\overline{\mathbf{B}} = \frac{1}{\det(\mathbf{J})} [J_{22} \quad -J_{12}] \begin{bmatrix} \frac{\partial \psi_1}{\partial \xi} & \frac{\partial \psi_2}{\partial \xi} & \frac{\partial \psi_3}{\partial \xi} & \frac{\partial \psi_4}{\partial \xi} & \frac{\partial \psi_5}{\partial \xi} & \frac{\partial \psi_6}{\partial \xi} & \frac{\partial \psi_7}{\partial \xi} & \frac{\partial \psi_8}{\partial \xi} \\ \frac{\partial \psi_1}{\partial \eta} & \frac{\partial \psi_2}{\partial \eta} & \frac{\partial \psi_3}{\partial \eta} & \frac{\partial \psi_4}{\partial \eta} & \frac{\partial \psi_5}{\partial \eta} & \frac{\partial \psi_6}{\partial \eta} & \frac{\partial \psi_7}{\partial \eta} & \frac{\partial \psi_8}{\partial \eta} \end{bmatrix}. \tag{4.18}$$

Taking into consideration the contribution of all elements, the effective coefficient is given in the form

$$C_{55}^* = \sum_e {}^eC_{55}^*. \tag{4.19}$$

4.1.3. Imperfect matrix

The contribution to the energy of the traction force appearing in the total potential energy Eq. (4.1) is

$$\Pi_T = \int_S u^T T \, dS. \tag{4.20}$$

Now, let us consider an edge $l_{1-5-2}^{(\Upsilon)}$ of an element, acted on by a traction $T = {}_{13}T_3^{(\Upsilon)}$ in the Υ phase (see, Fig. 3), and taking the element thickness t_e as constant over the element, we have

$$\Pi_T^{(\Upsilon)} = t_e \int_{l_{1-5-2}^{(\Upsilon)}} {}_{13}M_3^{(\Upsilon)} \, {}_{13}T_3^{(\Upsilon)} \, dl. \tag{4.21}$$

Using the interpolation relations involving the shape functions

$${}_{13}M_3^{(\Upsilon)} = \psi_1 q_{31}^{(\Upsilon)} + \psi_2 q_{32}^{(\Upsilon)} + \psi_5 q_{35}^{(\Upsilon)}, \tag{4.22}$$

$${}_{13}T_3^{(\Upsilon)} = \psi_1 T_{31}^{(\Upsilon)} + \psi_2 T_{32}^{(\Upsilon)} + \psi_5 T_{35}^{(\Upsilon)}, \tag{4.23}$$

where $q_{31}^{(\Upsilon)}$, $q_{32}^{(\Upsilon)}$, $q_{35}^{(\Upsilon)}$ ($T_{31}^{(\Upsilon)}, T_{32}^{(\Upsilon)}, T_{35}^{(\Upsilon)}$) are the displacements (tractions) in the Υ phase of the nodes 1, 2, 5 and ψ_1, ψ_2, ψ_5 are the shape functions given in Eq. (4.7) for $\eta = -1$ which coincide with one-dimensional quadratic shape functions

$$\begin{aligned} \psi_1 &= -0.5\,\xi(1-\xi), \\ \psi_2 &= 0.5\,\xi(1+\xi), \\ \psi_5 &= (1-\xi)(1+\xi). \end{aligned} \tag{4.24}$$

The imperfect contact condition given in Eq. (3.35) for the nodes 1, 2, 5 can be written

$$\begin{aligned} T_{31}^{(\Upsilon)} &= -\frac{\kappa_a C_{55}^{(2)}}{R} \left(q_{31}^{(\Upsilon)} - q_{32}^{(\varsigma)} \right), \\ T_{32}^{(\Upsilon)} &= -\frac{\kappa_a C_{55}^{(2)}}{R} \left(q_{32}^{(\Upsilon)} - q_{31}^{(\varsigma)} \right), \\ T_{35}^{(\Upsilon)} &= -\frac{\kappa_a C_{55}^{(2)}}{R} \left(q_{35}^{(\Upsilon)} - q_{35}^{(\varsigma)} \right), \end{aligned} \tag{4.25}$$

where $\varsigma = 1$ ($\varsigma = 2$) for $\Upsilon = 2$ ($\Upsilon = 1$). Now, the total potential energy associated to the traction force is written by the following expression,

$$\Pi_T^I = \frac{1}{2} \left(\Pi_T^{(1)} + \Pi_T^{(2)} \right). \tag{4.26}$$

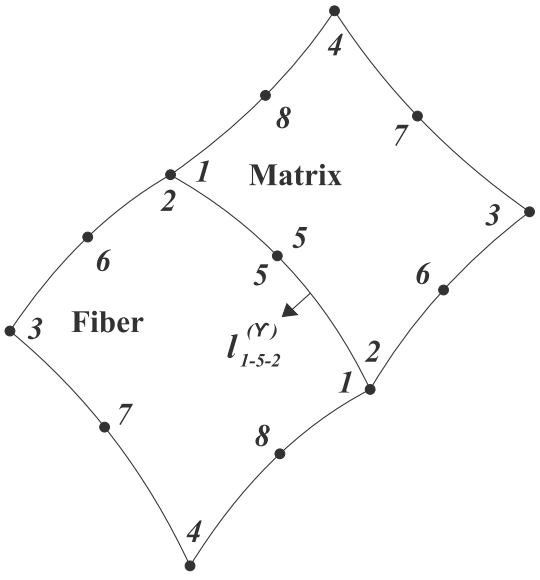

Fig. 3. Representation of two elements in the interface.

Using (4.21) for $\Upsilon = 1, 2$ and (4.26) then the total potential energy associated to traction force in matrix form is

$$\Pi_T^l = \frac{1}{2}\bar{\mathbf{q}}^T \mathbf{K}_T^l \bar{\mathbf{q}}, \tag{4.27}$$

where $\bar{\mathbf{q}}^T = \begin{bmatrix} q_{31}^{(2)} & q_{32}^{(2)} & q_{35}^{(2)} & q_{31}^{(1)} & q_{32}^{(1)} & q_{35}^{(1)} \end{bmatrix}$ and $\mathbf{K}_T^l$ is the imperfect matrix

$$\mathbf{K}_T^l = \frac{\kappa_a C_{55}^{(2)} t_e}{R} \begin{bmatrix} -I_{11} & -I_{12} & -I_{15} & I_{12} & I_{11} & I_{15} \\ & -I_{22} & -I_{25} & I_{22} & I_{21} & I_{25} \\ & & -I_{55} & I_{52} & I_{51} & I_{55} \\ & & & -I_{22} & -I_{12} & -I_{25} \\ & \textit{Symm} & & & -I_{11} & -I_{15} \\ & & & & & -I_{55} \end{bmatrix}. \tag{4.28}$$

Here

$$I_{ij} = I_{ji} = \int_{l_{1-5-2}^{(2)}} \psi_i \psi_j \, dl, \quad i,j = 1,2,5. \tag{4.29}$$

Considering all the contributions of the interface to traction potential energy, we have

$$\Pi_T = \sum_l \Pi_T^l = \frac{1}{2}\overline{\mathbf{Q}}^T \mathbf{K}_T \overline{\mathbf{Q}}, \tag{4.30}$$

where $\mathbf{K}_T(\overline{\mathbf{Q}})$ is the global imperfect matrix (global interface displacement vector).

The contribution to total potential energy is obtained adding strain potential energy and traction energy. Algebraic system of equations is obtained deriving the total potential energy with respect to the global displacement vector, equating them to zero and applying the boundary conditions. Using the solution of the algebraic system of equations the associated effective coefficient (4.19) for the antiplane problem ${}_{13}L$ is obtained. Similarly the antiplane problem ${}_{23}L$ can be solved.

4.2. The plane problem ${}_{11}L$

In a similar way we deal with the ${}_{11}L$ local problem. The relations ((3.43)–(3.45)) for $\beta\beta = 11$ can be written in matrix form as

$${}_{11}\sigma = \mathbf{D}\,{}_{11}\varepsilon, \tag{4.31}$$

where

$$\begin{aligned} &{}_{11}\sigma = \begin{bmatrix} {}_{11}\sigma_{11} & {}_{11}\sigma_{22} & {}_{11}\sigma_{12} \end{bmatrix}^T, \quad u = \begin{bmatrix} {}_{11}M_1 & {}_{11}M_2 \end{bmatrix}, \\ &{}_{11}\varepsilon = \begin{bmatrix} {}_{11}\varepsilon_{11} & {}_{11}\varepsilon_{22} & {}_{11}\varepsilon_{12} \end{bmatrix}^T = \begin{bmatrix} \frac{\partial_{11}M_1}{\partial y_1} & \frac{\partial_{11}M_2}{\partial y_2} & \frac{\partial_{11}M_2}{\partial y_1} + \frac{\partial_{11}M_1}{\partial y_2} \end{bmatrix}^T, \\ &\mathbf{D} = \begin{bmatrix} C_{11} & C_{12} & 0 \\ C_{12} & C_{11} & 0 \\ 0 & 0 & C_{66} \end{bmatrix}. \end{aligned} \tag{4.32}$$

Using the shape function (4.7) and nodal values of the unknown displacement field, the displacements within the quadrilateral element are now written as

$${}_{11}\mathbf{M} = \Psi \mathbf{q}, \tag{4.33}$$

where

$$\begin{aligned} &{}_{11}\mathbf{M} = \begin{bmatrix} {}_{11}M_1 & {}_{11}M_2 \end{bmatrix}^T, \\ &\Psi = \begin{bmatrix} \psi_1 & 0 & \psi_2 & 0 & \psi_3 & 0 & \psi_4 & 0 & \psi_5 & 0 & \psi_6 & 0 & \psi_7 & 0 & \psi_8 & 0 \\ 0 & \psi_1 & 0 & \psi_2 & 0 & \psi_3 & 0 & \psi_4 & 0 & \psi_5 & 0 & \psi_6 & 0 & \psi_7 & 0 & \psi_8 \end{bmatrix}, \\ &\mathbf{q} = \begin{bmatrix} q_{11} & q_{21} & q_{12} & q_{22} & q_{13} & q_{23} & q_{14} & q_{24} & q_{15} & q_{25} & q_{16} & q_{26} & q_{17} & q_{27} & q_{18} & q_{28} \end{bmatrix}^T, \end{aligned} \tag{4.34}$$

$${}_{11}\varepsilon = \begin{bmatrix} \frac{\partial_{11}M_1}{\partial y_1} \\ \frac{\partial_{11}M_2}{\partial y_2} \\ \frac{\partial_{11}M_2}{\partial y_1} + \frac{\partial_{11}M_1}{\partial y_2} \end{bmatrix} = \frac{1}{\det(\mathbf{J})} \begin{bmatrix} J_{22} & -J_{12} & 0 & 0 \\ 0 & 0 & -J_{21} & J_{11} \\ -J_{21} & J_{11} & J_{22} & -J_{12} \end{bmatrix} \begin{bmatrix} \frac{\partial_{11}M_1}{\partial \xi} \\ \frac{\partial_{11}M_1}{\partial \eta} \\ \frac{\partial_{11}M_2}{\partial \xi} \\ \frac{\partial_{11}M_2}{\partial \eta} \end{bmatrix}. \tag{4.35}$$

Using (4.31) and (4.33) the strain can be written in matrix form as

$${}_{11}\varepsilon = \mathbf{B}\mathbf{q}, \tag{4.36}$$

where

$$\mathbf{B} = \frac{1}{\det(\mathbf{J})} \begin{bmatrix} J_{22} & -J_{12} & 0 & 0 \\ 0 & 0 & -J_{21} & J_{11} \\ -J_{21} & J_{11} & J_{22} & -J_{12} \end{bmatrix} \times \begin{bmatrix} \frac{\partial\psi_1}{\partial\xi} & 0 & \frac{\partial\psi_2}{\partial\xi} & 0 & \frac{\partial\psi_3}{\partial\xi} & 0 & \frac{\partial\psi_4}{\partial\xi} & 0 & \frac{\partial\psi_5}{\partial\xi} & 0 & \frac{\partial\psi_6}{\partial\xi} & 0 & \frac{\partial\psi_7}{\partial\xi} & 0 & \frac{\partial\psi_8}{\partial\xi} & 0 \\ \frac{\partial\psi_1}{\partial\eta} & 0 & \frac{\partial\psi_2}{\partial\eta} & 0 & \frac{\partial\psi_3}{\partial\eta} & 0 & \frac{\partial\psi_4}{\partial\eta} & 0 & \frac{\partial\psi_5}{\partial\eta} & 0 & \frac{\partial\psi_6}{\partial\eta} & 0 & \frac{\partial\psi_7}{\partial\eta} & 0 & \frac{\partial\psi_8}{\partial\eta} & 0 \\ 0 & \frac{\partial\psi_1}{\partial\xi} & 0 & \frac{\partial\psi_2}{\partial\xi} & 0 & \frac{\partial\psi_3}{\partial\xi} & 0 & \frac{\partial\psi_4}{\partial\xi} & 0 & \frac{\partial\psi_5}{\partial\xi} & 0 & \frac{\partial\psi_6}{\partial\xi} & 0 & \frac{\partial\psi_7}{\partial\xi} & 0 & \frac{\partial\psi_8}{\partial\xi} \\ 0 & \frac{\partial\psi_1}{\partial\eta} & 0 & \frac{\partial\psi_2}{\partial\eta} & 0 & \frac{\partial\psi_3}{\partial\eta} & 0 & \frac{\partial\psi_4}{\partial\eta} & 0 & \frac{\partial\psi_5}{\partial\eta} & 0 & \frac{\partial\psi_6}{\partial\eta} & 0 & \frac{\partial\psi_7}{\partial\eta} & 0 & \frac{\partial\psi_8}{\partial\eta} \end{bmatrix}. \tag{4.36}$$

Consequently, from (4.31) and (4.36) we obtain the stress matrix

$${}_{11}\sigma = \mathbf{D}\mathbf{B}\mathbf{q}. \tag{4.37}$$

4.2.1. Element stiffness matrix

Replacing (4.37) and (4.36) into (4.13) the strain energy associated to one plane element is obtained

$$\Pi_S^e = \frac{1}{2}\mathbf{q}^T \mathbf{K}_S^e \mathbf{q}, \tag{4.38}$$

where $\mathbf{K}_S^e$ is the element stiffness matrix given by

$$\mathbf{K}_S^e = t_e \int_{-1}^{1}\int_{-1}^{1} \mathbf{B}^T \mathbf{D}\mathbf{B} \det(\mathbf{J}) \, d\xi \, d\eta. \tag{4.39}$$

Considering the contribution of all the elements to strain potential energy we obtain

$$\Pi_S = \frac{1}{2}\mathbf{Q}^T \mathbf{K}_S \mathbf{Q}, \tag{4.40}$$

where $\mathbf{K}_S$ $(\mathbf{Q})$ is the global stiffness matrix (global displacement vector).

4.2.2. Effective coefficient

Now, replacing the derivatives $\partial_{11}M_1/\partial y_1, \partial_{11}M_2/\partial y_2$ which are involved in (4.35) and the relation (4.33) into the expressions C_{11}^*, C_{21}^*, C_{31}^* given in (3.52), we obtain the contribution of element (e) in the effective coefficients

$${}^e\mathbf{C}^* = 4\int_{-1}^{1}\int_{-1}^{1} \overline{\mathbf{D}}\overline{\mathbf{B}}\mathbf{q} \det(\mathbf{J}) \, d\xi \, d\eta, \tag{4.41}$$

where

$$\begin{aligned} &{}^e\mathbf{C}^* = \begin{bmatrix} {}^eC_{11}^* & {}^eC_{21}^* & {}^eC_{31}^* \end{bmatrix}^T, \\ &\overline{\mathbf{B}} = \frac{1}{\det(\mathbf{J})} \begin{bmatrix} J_{22} & -J_{12} & 0 & 0 \\ 0 & 0 & -J_{21} & J_{11} \\ J_{22} & -J_{12} & -J_{21} & J_{11} \end{bmatrix} \\ &\quad \times \begin{bmatrix} \frac{\partial\psi_1}{\partial\xi} & 0 & \frac{\partial\psi_2}{\partial\xi} & 0 & \frac{\partial\psi_3}{\partial\xi} & 0 & \frac{\partial\psi_4}{\partial\xi} & 0 & \frac{\partial\psi_5}{\partial\xi} & 0 & \frac{\partial\psi_6}{\partial\xi} & 0 & \frac{\partial\psi_7}{\partial\xi} & 0 & \frac{\partial\psi_8}{\partial\xi} & 0 \\ \frac{\partial\psi_1}{\partial\eta} & 0 & \frac{\partial\psi_2}{\partial\eta} & 0 & \frac{\partial\psi_3}{\partial\eta} & 0 & \frac{\partial\psi_4}{\partial\eta} & 0 & \frac{\partial\psi_5}{\partial\eta} & 0 & \frac{\partial\psi_6}{\partial\eta} & 0 & \frac{\partial\psi_7}{\partial\eta} & 0 & \frac{\partial\psi_8}{\partial\eta} & 0 \\ 0 & \frac{\partial\psi_1}{\partial\xi} & 0 & \frac{\partial\psi_2}{\partial\xi} & 0 & \frac{\partial\psi_3}{\partial\xi} & 0 & \frac{\partial\psi_4}{\partial\xi} & 0 & \frac{\partial\psi_5}{\partial\xi} & 0 & \frac{\partial\psi_6}{\partial\xi} & 0 & \frac{\partial\psi_7}{\partial\xi} & 0 & \frac{\partial\psi_8}{\partial\xi} \\ 0 & \frac{\partial\psi_1}{\partial\eta} & 0 & \frac{\partial\psi_2}{\partial\eta} & 0 & \frac{\partial\psi_3}{\partial\eta} & 0 & \frac{\partial\psi_4}{\partial\eta} & 0 & \frac{\partial\psi_5}{\partial\eta} & 0 & \frac{\partial\psi_6}{\partial\eta} & 0 & \frac{\partial\psi_7}{\partial\eta} & 0 & \frac{\partial\psi_8}{\partial\eta} \end{bmatrix}, \end{aligned} \tag{4.41}$$

$$\overline{\mathbf{D}} = \begin{bmatrix} {}^{e}C_{11} & {}^{e}C_{12} & 0 \\ {}^{e}C_{12} & {}^{e}C_{11} & 0 \\ 0 & 0 & {}^{e}C_{13} \end{bmatrix}.$$

The effective coefficients taking into account the contribution of all elements can be given in the form

$$C^{*}_{11} = \sum_{e} {}^{e}C^{*}_{11}, \quad C^{*}_{21} = \sum_{e} {}^{e}C^{*}_{21}, \quad C^{*}_{31} = \sum_{e} {}^{e}C^{*}_{31}. \tag{4.42}$$

4.2.3. Imperfect matrix

Consider an edge $l^{(\Upsilon)}_{1-5-2}$ (see, Fig. 3) acted on by a traction $T = [{}_{11}T^{(\Upsilon)}_{1} \;\; {}_{11}T^{(\Upsilon)}_{2}]$ and taking the element thickness t_e as constant over the element, the potential energy $\Pi^{(\Upsilon)}_{T}$ of the traction for the Υ phase is

$$\Pi^{(\Upsilon)}_{T} = t_e \int_{l^{(\Upsilon)}_{1-5-2}} \left({}_{11}M^{(\Upsilon)}_{1} \, {}_{11}T^{(\Upsilon)}_{1} + {}_{11}M^{(\Upsilon)}_{2} \, {}_{11}T^{(\Upsilon)}_{2} \right) dl. \tag{4.43}$$

The displacements $({}_{11}M^{(\Upsilon)}_{1}, {}_{11}M^{(\Upsilon)}_{2})$ and the tractions $({}_{11}T^{(\Upsilon)}_{1}, {}_{11}T^{(\Upsilon)}_{2})$ in the Υ phase are related to the shape functions by means of

$${}_{11}M^{(\Upsilon)}_{1} = \psi_1 q^{(\Upsilon)}_{11} + \psi_2 q^{(\Upsilon)}_{12} + \psi_5 q^{(\Upsilon)}_{15}, \tag{4.44}$$

$${}_{11}M^{(\Upsilon)}_{2} = \psi_1 q^{(\Upsilon)}_{21} + \psi_2 q^{(\Upsilon)}_{22} + \psi_5 q^{(\Upsilon)}_{25}, \tag{4.45}$$

$${}_{11}T^{(\Upsilon)}_{1} = \psi_1 T^{(\Upsilon)}_{11} + \psi_2 T^{(\Upsilon)}_{12} + \psi_5 T^{(\Upsilon)}_{15}, \tag{4.46}$$

$${}_{11}T^{(\Upsilon)}_{2} = \psi_1 T^{(\Upsilon)}_{21} + \psi_2 T^{(\Upsilon)}_{22} + \psi_5 T^{(\Upsilon)}_{25}, \tag{4.47}$$

where $q^{(\Upsilon)}_{11}$, $q^{(\Upsilon)}_{12}$, $q^{(\Upsilon)}_{15}$ and $T^{(\Upsilon)}_{11}$, $T^{(\Upsilon)}_{12}$, $T^{(\Upsilon)}_{15}$ ($q^{(\Upsilon)}_{21}, q^{(\Upsilon)}_{22}, q^{(\Upsilon)}_{25}$ and $T^{(\Upsilon)}_{21}, T^{(\Upsilon)}_{22}, T^{(\Upsilon)}_{25}$) are the displacements and tractions in the y_1 (y_2)-direction for the phase Υ of the nodes 1, 2 and 5, respectively. The shape functions ψ_1, ψ_2, ψ_5 are given in (4.24). The tractions in the nodes 1, 2 and 5 can be calculated by

$$T^{(\Upsilon)}_{1\iota} = \sin(\theta) T^{(\Upsilon)}_{t\iota} + \cos(\theta) T^{(\Upsilon)}_{n\iota}, \tag{4.48}$$

$$T^{(\Upsilon)}_{2\iota} = -\cos(\theta) T^{(\Upsilon)}_{t\iota} + \sin(\theta) T^{(\Upsilon)}_{n\iota}, \tag{4.49}$$

here θ is the angle between the unit normal vector with y_1-direction; $T^{(\Upsilon)}_{t\iota}$ ($T^{(\Upsilon)}_{n\iota}$) is the tangential (normal) traction in the Υ phase for the $\iota = 1, 2, 5$ nodes given by

$$T^{(\Upsilon)}_{t1} = -\frac{\kappa_t C^{(2)}_{55}}{R}\left(q^{(\Upsilon)}_{t1} - q^{(\varsigma)}_{t2}\right), \quad T^{(\Upsilon)}_{t2} = -\frac{\kappa_t C^{(2)}_{55}}{R}\left(q^{(\Upsilon)}_{t2} - q^{(\varsigma)}_{t1}\right), \tag{4.50}$$

$$T^{(\Upsilon)}_{t5} = -\frac{\kappa_t C^{(2)}_{55}}{R}\left(q^{(\Upsilon)}_{t5} - q^{(\varsigma)}_{t5}\right), \quad T^{(\Upsilon)}_{n1} = -\frac{\kappa_n C^{(2)}_{55}}{R}\left(q^{(\varsigma)}_{n1} - q^{(\Upsilon)}_{n2}\right), \tag{4.51}$$

$$T^{(\Upsilon)}_{n2} = -\frac{\kappa_n C^{(2)}_{55}}{R}\left(q^{(\Upsilon)}_{n2} - q^{(\varsigma)}_{n1}\right), \quad T^{(\Upsilon)}_{n5} = -\frac{\kappa_n C^{(2)}_{55}}{R}\left(q^{(\Upsilon)}_{n5} - q^{(\varsigma)}_{n5}\right), \tag{4.52}$$

where $\varsigma = 1$ ($\varsigma = 2$) for $\Upsilon = 2$ ($\Upsilon = 1$) and the tangential (normal) displacement in the $\iota = 1, 2, 5$ nodes is $q^{(\Upsilon)}_{t\iota} = \sin(\theta) q^{(\Upsilon)}_{1\iota} - \cos(\theta) q^{(\Upsilon)}_{2\iota}$ $\left(q^{(\Upsilon)}_{n\iota} = \cos(\theta) q^{(\Upsilon)}_{1\iota} + \sin(\theta) q^{(\Upsilon)}_{2\iota}\right)$ for each phase $\Upsilon = 1, 2$.

Now, we can write the total potential energy associated to the traction force by the following expression,

$$\Pi^{I}_{T} = \frac{1}{2}\left(\Pi^{(1)}_{T} + \Pi^{(2)}_{T}\right). \tag{4.53}$$

Using (4.43) for $\Upsilon = 1, 2$ and (4.53) then the total potential energy associated to traction force in matrix form is

$$\Pi^{I}_{T} = \frac{1}{2}\bar{\mathbf{q}}^{T}\mathbf{K}^{I}_{T}\bar{\mathbf{q}}, \tag{4.54}$$

where $\bar{\mathbf{q}}^{T} = \left[q^{(2)}_{11} \; q^{(2)}_{21} \; q^{(2)}_{12} \; q^{(2)}_{22} \; q^{(2)}_{15} \; q^{(2)}_{25} q^{(1)}_{11} \; q^{(1)}_{21} \; q^{(1)}_{12} \; q^{(1)}_{22} \; q^{(1)}_{15} \; q^{(1)}_{25}\right]$,

$$\mathbf{K}^{I}_{T} = \frac{\kappa_t C^{(2)}_{55}}{R}\mathbf{P} + \frac{\kappa_n C^{(2)}_{55}}{R}\mathbf{Q}, \tag{4.55}$$

and

$$\mathbf{P} = \begin{pmatrix}
-F^{2211}_{2212} & F^{2211}_{2112} & -F^{2221}_{2212} & F^{2221}_{2112} & -F^{2251}_{2212} & F^{2251}_{1212} & F^{2121}_{2221} & -F^{2121}_{2121} & F^{2111}_{2221} & -F^{2111}_{2121} & F^{2151}_{2221} & -F^{2151}_{1221} \\
 & -F^{2211}_{1112} & F^{2221}_{2112} & -F^{2221}_{1112} & F^{2251}_{2112} & -F^{2251}_{1112} & F^{2121}_{1221} & F^{2121}_{1121} & -F^{2111}_{1221} & F^{2111}_{1121} & -F^{2151}_{1221} & F^{2151}_{1121} \\
 & & -F^{2222}_{2212} & F^{2222}_{2112} & -F^{2225}_{2212} & F^{2225}_{1212} & F^{2122}_{2221} & -F^{2122}_{2121} & F^{2121}_{2221} & -F^{2121}_{2121} & F^{2125}_{2221} & -F^{2125}_{2121} \\
 & & & -F^{2222}_{1112} & F^{2225}_{2112} & -F^{2225}_{1112} & F^{2122}_{1221} & F^{2122}_{1121} & -F^{2121}_{1221} & F^{2121}_{1121} & -F^{2125}_{1221} & F^{2125}_{1121} \\
 & & & & -F^{2255}_{2212} & F^{2255}_{2112} & F^{2125}_{2221} & -F^{2125}_{2121} & F^{2151}_{2221} & -F^{2151}_{2121} & F^{2155}_{2221} & -F^{2155}_{2121} \\
 & & & & & -F^{2255}_{1112} & F^{2125}_{1221} & F^{2125}_{1121} & -F^{2151}_{1221} & F^{2151}_{1121} & -F^{2155}_{1221} & F^{2155}_{1121} \\
 & & & & & & -G^{1122}_{2212} & G^{1122}_{2112} & -G^{1112}_{2212} & G^{1112}_{2112} & -G^{1152}_{2212} & G^{1152}_{2112} \\
 & & & & & & & -G^{1122}_{1112} & G^{1112}_{2112} & -G^{1112}_{1112} & G^{1152}_{2112} & -G^{1152}_{1112} \\
 & & & & & & & & -G^{1111}_{2212} & G^{1111}_{2112} & -G^{1115}_{2212} & G^{1115}_{2112} \\
 & & & & & & & & & -G^{1111}_{1112} & G^{1115}_{2112} & -G^{1115}_{1112} \\
 & & & & & & & & & & -G^{1155}_{2212} & G^{1155}_{2112} \\
 & & & & & & & & & & & -G^{1155}_{1112}
\end{pmatrix}$$

Symm

$$\mathbf{Q} = \begin{pmatrix}
-F^{2211}_{1112} & -F^{2211}_{1212} & -F^{2221}_{1112} & -F^{2221}_{1212} & -F^{2251}_{1112} & -F^{2251}_{2112} & F^{2121}_{1121} & F^{2121}_{1221} & F^{2111}_{1121} & F^{2111}_{1221} & F^{2151}_{1121} & F^{2151}_{1221} \\
 & -F^{2211}_{2212} & -F^{2221}_{1212} & -F^{2221}_{2212} & -F^{2251}_{1212} & -F^{2251}_{2212} & F^{2121}_{2121} & F^{2121}_{2221} & F^{2111}_{2121} & F^{2111}_{2221} & F^{2151}_{2121} & F^{2151}_{2221} \\
 & & -F^{2222}_{1112} & -F^{2222}_{1212} & -F^{2225}_{1112} & -F^{2225}_{2112} & F^{2122}_{1121} & F^{2122}_{1221} & F^{2121}_{1121} & F^{2121}_{1221} & F^{2125}_{1121} & F^{2125}_{1221} \\
 & & & -F^{2222}_{2212} & -F^{2225}_{1212} & -F^{2225}_{2212} & F^{2122}_{2121} & F^{2122}_{2221} & F^{2121}_{2121} & F^{2121}_{2221} & F^{2125}_{2121} & F^{2125}_{2221} \\
 & & & & -F^{2255}_{1112} & -F^{2255}_{1212} & F^{2125}_{1121} & F^{2125}_{1221} & F^{2151}_{1121} & F^{2151}_{1221} & F^{2155}_{1121} & F^{2155}_{1221} \\
 & & & & & -F^{2255}_{2212} & F^{2125}_{2121} & F^{2125}_{2221} & F^{2151}_{2121} & F^{2151}_{2221} & F^{2155}_{2121} & F^{2155}_{2221} \\
 & & & & & & -G^{1122}_{1112} & -G^{1122}_{1212} & -G^{1112}_{1112} & -G^{1112}_{1212} & -G^{1152}_{1112} & -G^{1152}_{1212} \\
 & & & & & & & -G^{1122}_{2212} & -G^{1112}_{1212} & -G^{1112}_{2212} & -G^{1152}_{1212} & -G^{1152}_{2212} \\
 & & & & & & & & -G^{1111}_{1112} & -G^{1111}_{1212} & -G^{1115}_{1112} & -G^{1115}_{1212} \\
 & & & & & & & & & -G^{1111}_{2212} & -G^{1115}_{1212} & -G^{1115}_{2212} \\
 & & & & & & & & & & -G^{1155}_{1112} & -G^{1155}_{1212} \\
 & & & & & & & & & & & -G^{1155}_{2212}
\end{pmatrix}$$

Symm

$$F_{ijkl}^{nm\alpha\beta} = {}^{\alpha\beta}\Pi_{i112}^{(n)}\bar{y}_{jk}^{(m)} + {}^{\alpha\beta}\Pi_{i212}^{(n)}\bar{y}_{jl}^{(m)} + {}^{\alpha\beta}\Pi_{i512}^{(n)}\bar{y}_{j5}^{(m)}, \tag{4.56}$$

$$G_{ijkl}^{nm\alpha\beta} = {}^{\alpha\beta}\Pi_{i221}^{(n)}\bar{y}_{jk}^{(m)} + {}^{\alpha\beta}\Pi_{i121}^{(n)}\bar{y}_{jl}^{(m)} + {}^{\alpha\beta}\Pi_{i521}^{(n)}\bar{y}_{j5}^{(m)}, \tag{4.57}$$

$${}^{\alpha\beta}\Pi_{i\gamma\xi\eta}^{(n)} = {}^{\alpha\beta}I_{\xi\gamma}\bar{y}_{i1}^{(n)} + {}^{\alpha\beta}I_{\eta\gamma}\bar{y}_{i2}^{(n)} + {}^{\alpha\beta}I_{5\gamma}\bar{y}_{i5}^{(n)}, \tag{4.58}$$

$${}^{\alpha\beta}I_{\xi\gamma} = t_e \int_{l_{1-5-2}^{(2)}} \psi_\xi \psi_\gamma \psi_\alpha \psi_\beta \, dl, \tag{4.59}$$

where $\bar{y}_{ij} = y_{ij}/R$, $i, j, k, l, n, m = 1,2$, and $\xi, \gamma, \alpha, \beta = 1,2,5$. In the expression (4.55) we have considered the following relations $cos(\theta) = y_1/R$, $sin(\theta) = y_2/R$, $y_1 = \psi_1 y_{11} + \psi_5 y_{15} + \psi_2 y_{12}$ and $y_2 = \psi_1 y_{21} + \psi_5 y_{25} + \psi_2 y_{22}$.

The contribution of the interface to traction potential energy is given by the expression

$$\Pi_T = \sum_l \Pi_T^l = \frac{1}{2}\overline{\mathbf{Q}}^T \mathbf{K}_T \overline{\mathbf{Q}}, \tag{4.60}$$

where $\mathbf{K}_T(\overline{\mathbf{Q}})$ is the global imperfect matrix (global interface displacement vector).

The contribution to total potential energy is obtained by addition of the strain potential energy and traction energy. An algebraic system of equations is obtained deriving the total potential energy with respect to the global displacement vector $\mathbf{Q}$, equating them to zero and applying the boundary conditions. Using the solution of the algebraic system of equations, the associated effective coefficient (4.42) to plane problem ${}_{11}L$ is obtained. Analogously, the plane problems ${}_{22}L$, ${}_{12}L$ can be solved.

5. Numerical results

The following elastic constants have been used throughout in the numerical calculations: $E^{(2)} = 70$ GPa (Young's modulus) and $\nu^{(2)} = 0.3$ (Poisson's ratio) for the matrix, and $E^{(1)} = 450$ GPa and $\nu^{(1)} = 0.17$ for the fiber.

Some limit cases are studied in order to validate our approach. For example, in Table 2 the set of all effective elastic coefficients are presented for different values of the fiber volume fraction γ_1. A comparison between the present model for $\kappa_a = \kappa_t = \kappa_n = 0$ and the analytical expressions of the effective coefficients for empty fibers obtained by asymptotic homogenization approach (Sabina et al., 2002) is given. It can be noticed a very good

Table 2
Effective coefficients C_{ij}^*(GPa) for $\kappa_a = \kappa_t = \kappa_n = 0$.

γ_1	C_{11}^*-Present model	C_{11}^*-Analytical	C_{12}^*-Present model	C_{12}^*-Analytical
0.05	80.525367267475	80.525340039910	33.149806825864	33.149802552080
0.20	53.390014041054	53.390011091840	18.365994181923	18.365993438240
0.35	36.536035848067	36.536034852230	9.781059283943	9.781059178809
0.55	20.498584257763	20.498583869870	3.378678373826	3.378679162697
0.75	5.849941587920	5.849968639273	0.289122177387	0.289123725301
	C_{13}^*-Present model	C_{13}^*-Analytical	C_{33}^*-Present model	C_{33}^*-Analytical
0.05	34.102552228002	34.102542777600	86.961531878495	86.961525666560
0.20	21.526802466893	21.526801359020	68.916081923221	68.916080815410
0.35	13.895128539603	13.895128209310	53.837077459125	53.837076925590
0.55	7.163178789477	7.163178909770	35.797907446184	35.797907345860
0.75	1.841719129592	1.841727709372	18.605034667715	18.605036625620
	C_{44}^*-Present model	C_{44}^*-Analytical	C_{66}^*-Present model	C_{66}^*-Analytical
0.05	24.358970441296	24.358969691260	23.209442250086	23.209425304530
0.20	17.945057074195	17.945056708350	13.422077906961	13.422075628730
0.35	12.915297272467	12.915297045270	6.616326760747	6.616325536051
0.55	7.459089293901	7.459089118081	1.808770619416	1.808766466272
0.75	2.111431016424	2.111428077125	0.078900908542	0.078817876229

Table 3
Normalized effective coefficients $\overline{C}_{ij}$ for $\kappa_a = \kappa_t = \kappa_n = \infty$.

γ_1	$\overline{C}_{11}$-Present model	$\overline{C}_{11}$-Analytical	$\overline{C}_{12}$-Present model	$\overline{C}_{12}$-Analytical
0.05	1.055613195746	1.055613441112	1.040485293402	1.040483818823
0.20	1.260696273098	1.260704666692	1.156459827399	1.156485577346
0.35	1.543615667429	1.543584712192	1.259934265506	1.259936217747
0.55	2.114481246274	2.114487722074	1.395770805810	1.395764597872
0.75	3.126404413003	3.126400805895	1.785169589159	1.785150605411
	$\overline{C}_{13}$-Present model	$\overline{C}_{13}$-Analytical	$\overline{C}_{33}$-Present model	$\overline{C}_{33}$-Analytical
0.05	1.022294039366	1.022293921242	1.200995351432	1.200995459529
0.20	1.100143613682	1.100149550268	1.805212872676	1.805213569382
0.35	1.200139066138	1.200129863461	2.411916019504	2.411915003437
0.55	1.392353788874	1.392354954620	3.227463196494	3.227463338156
0.75	1.752536715912	1.752533127859	4.061863498663	4.061863103712
	$\overline{C}_{44}$-Present model	$\overline{C}_{44}$-Analytical	$\overline{C}_{66}$-Present model	$\overline{C}_{66}$-Analytical
0.05	1.078377140607	1.078395713051	1.062477573412	1.062476469054
0.20	1.355509551192	1.355488493290	1.261921629590	1.261942999424
0.35	1.720073829280	1.720078399086	1.504115686223	1.504107158517
0.55	2.458415214418	2.458433864300	2.005299536116	2.005303251731
0.75	4.044105820407	4.044095981454	3.335487513251	3.335494113348

Table 4
Normalized effective coefficient $\overline{C}_{44}$

κ_a	5	5	10	10
γ_1	$\overline{C}_{44}$-Present model	$\overline{C}_{44}$-Analytical	$\overline{C}_{44}$-Present model	$\overline{C}_{44}$-Analytical
0.05	1.050497283000	1.050497329395	1.063227927489	1.063227983128
0.20	1.218551766000	1.218551776258	1.279448900256	1.279448911100
0.35	1.416761447000	1.416761454190	1.546963064155	1.546963086275
0.55	1.745183922000	1.745184682879	2.027389195300	2.027397880582
0.75	2.184697494000	2.184743450944	2.778602364788	2.779576843989
κ_a	50	50	∞	∞
γ_1	$\overline{C}_{44}$-Present model	$\overline{C}_{44}$-Analytical	$\overline{C}_{44}$-Present model	$\overline{C}_{44}$-Analytical
0.05	1.075134177545	1.075134240093	1.078377140607	1.078395713051
0.20	1.338803259987	1.338803271256	1.355509551192	1.355488493290
0.35	1.681006228453	1.681006257241	1.720073829280	1.720078399086
0.55	2.354450215382	2.354464076114	2.458415214418	2.458433863448
0.75	3.675314446315	3.677499910115	4.044105820407	4.043962317514

coincidence between the two approaches. The three imperfect parameters $(\kappa_a, \kappa_t, \kappa_n)$ involved in the semi-analytic method for analyzing the non-perfect adherence of the composite can be considered as an alternative computing form for describing the behavior of porous composite materials. Besides, all normalized effective elastic coefficients $(\overline{C}_{11} = C^*_{11}/C^{(2)}_{11}, \overline{C}_{12} = C^*_{12}/C^{(2)}_{12}, \overline{C}_{13} = C^*_{13}/C^{(2)}_{12}, \overline{C}_{33} = C^*_{33}/C^{(2)}_{11}, \overline{C}_{44} = C^*_{44}/C^{(2)}_{44}, \overline{C}_{66} = C^*_{66}/C^{(2)}_{44})$ for perfect contact between the matrix and fibers are calculated using the present model for $\kappa_a = \kappa_t = \kappa_n = \infty$ and Table 3 reports the results. A comparison between the present model and the analytical results obtained by asymptotic homogenization technique (Guinovart-Diaz et al., 2002) is presented. Both methods reproduce almost the same values in the whole range of volume fractions.

Table 4 shows the normalized effective coefficient $\overline{C}_{44} = C^*_{44}/C^{(2)}_{44}$ computed by the present model for different values of the fiber volume fraction γ_1 and axial imperfect parameter $(\kappa_a = 5, 10, 50, \infty)$. Good match between the present model and the analytical formulae derived by asymptotic homogenization technique (Lopez-Realpozo et al., 2011) is obtained.

Fig. 4 exhibits the normalized effective coefficient $C^*_{11}/C^{(2)}_{11}$ with respect to the fiber volume fraction for different values of the tangential imperfect parameter $\kappa_t = 0; 1; 5; 10; 20; 50; \infty$ and some fixed normal imperfect parameters $\kappa_n = 10; 20; 50; \infty$. The behavior of this coefficient increases monotonically as κ_t increases in all the range of the fiber volume fraction. Notice that, for bigger values of the normal tangential parameter κ_n, this property in the composite gets stronger and, near to percolation limit, the property becomes more compact, i.e. the curves are less spaced (Fig. 4(d)). The curvature of the curves for $\kappa_n = 10$ are not as pronounced as for $\kappa_n = \infty$. On the other hand, the effective properties converge to the property for tangential perfect contact as the

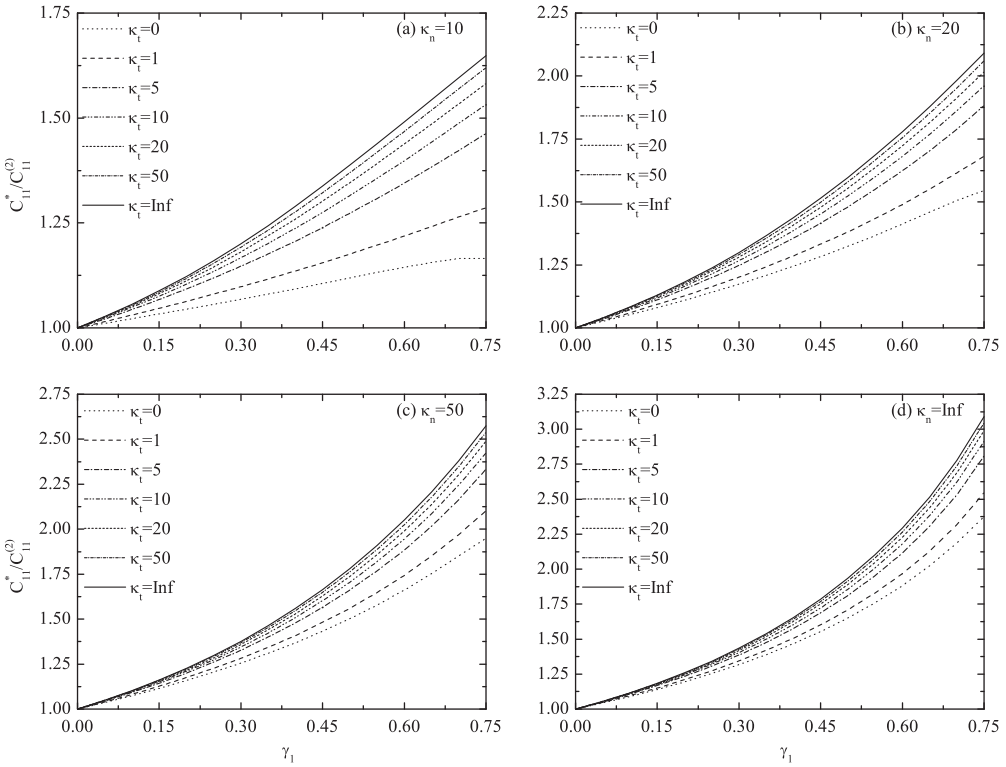

Fig. 4. Normalized effective coefficient $C^*_{11}/C^{(2)}_{11}$ versus fiber volume fraction γ_1 for different values of the imperfect parameters.

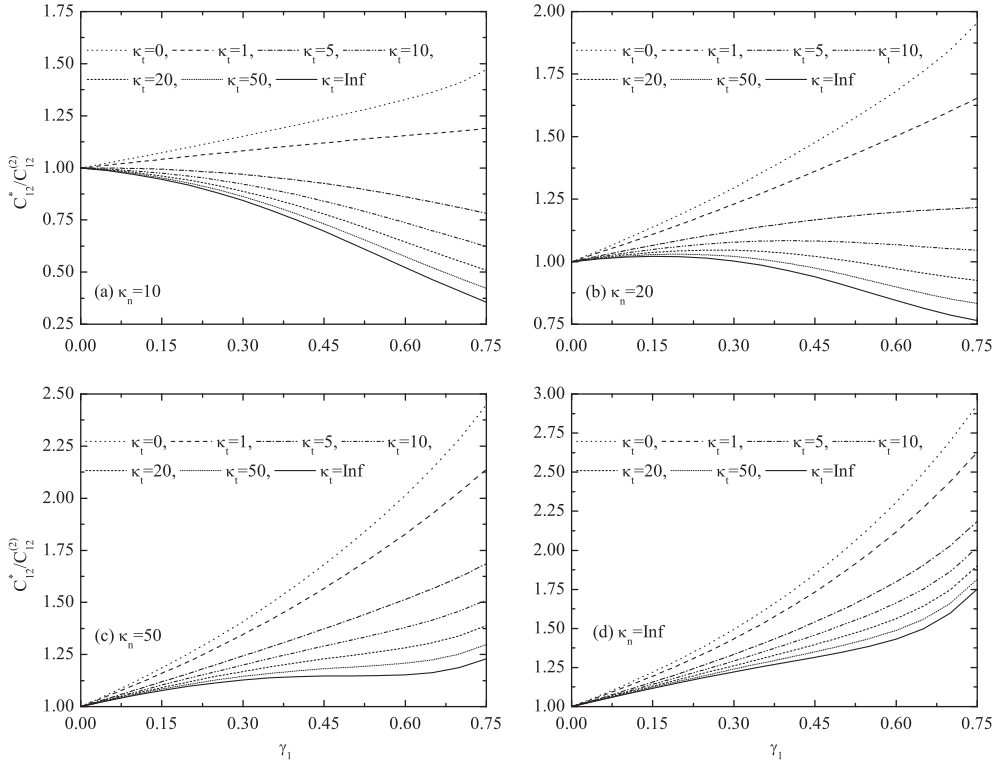

Fig. 5. Normalized effective coefficient $C^*_{12}/C^{(2)}_{12}$ versus fiber volume fraction γ_1 for different values of the imperfect parameters.

imperfection parameter κ_t approaches to ∞. Numerical results have shown that the imperfect parameters (κ_t, κ_n) have a significant effect on the coefficient $C^*_{11}/C^{(2)}_{11}$.

Fig. 5 displays the normalized effective coefficient $C^*_{12}/C^{(2)}_{12}$ with respect to the fiber volume fraction for different values of the tangential imperfect parameter $\kappa_t = 0; 1; 5; 10; 20; 50; \infty$ and some fixed normal imperfect parameters $\kappa_n = 10; 20; 50; \infty$. The behavior of this coefficient is different in comparison with the previous case. The contribution of $\kappa_n = 10; 20$ induces a decreasing behavior with the exception of some small values of the tangential imperfect

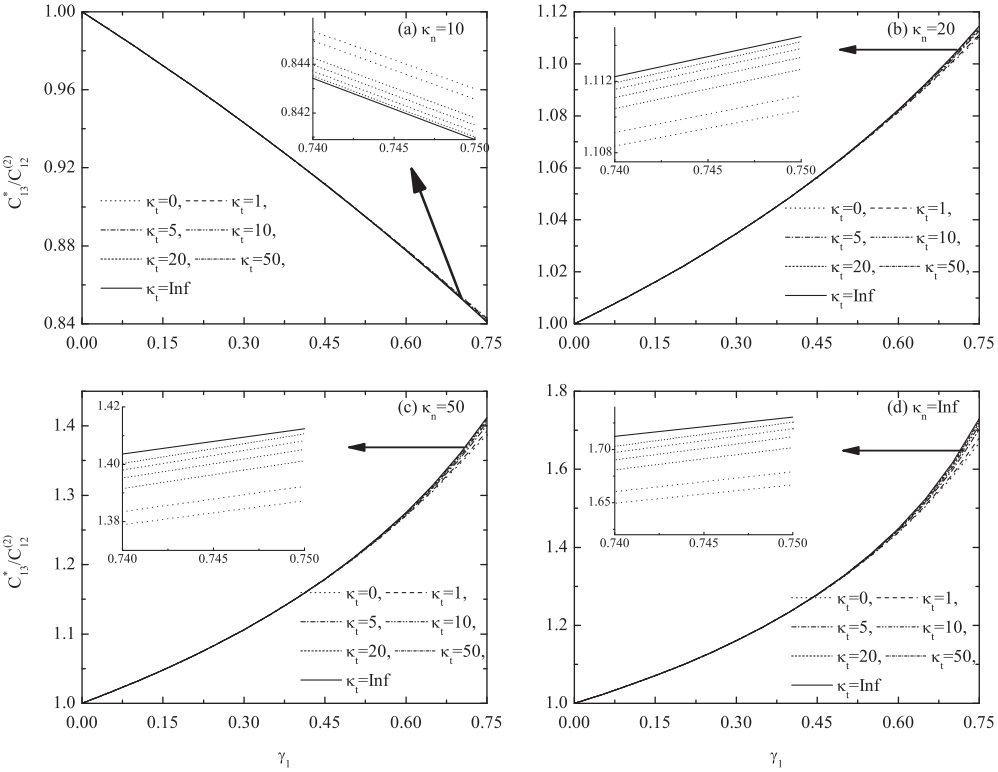

Fig. 6. Normalized effective coefficient $C^*_{13}/C^{(2)}_{12}$ versus fiber volume fraction γ_1 for different values of the imperfect parameters.

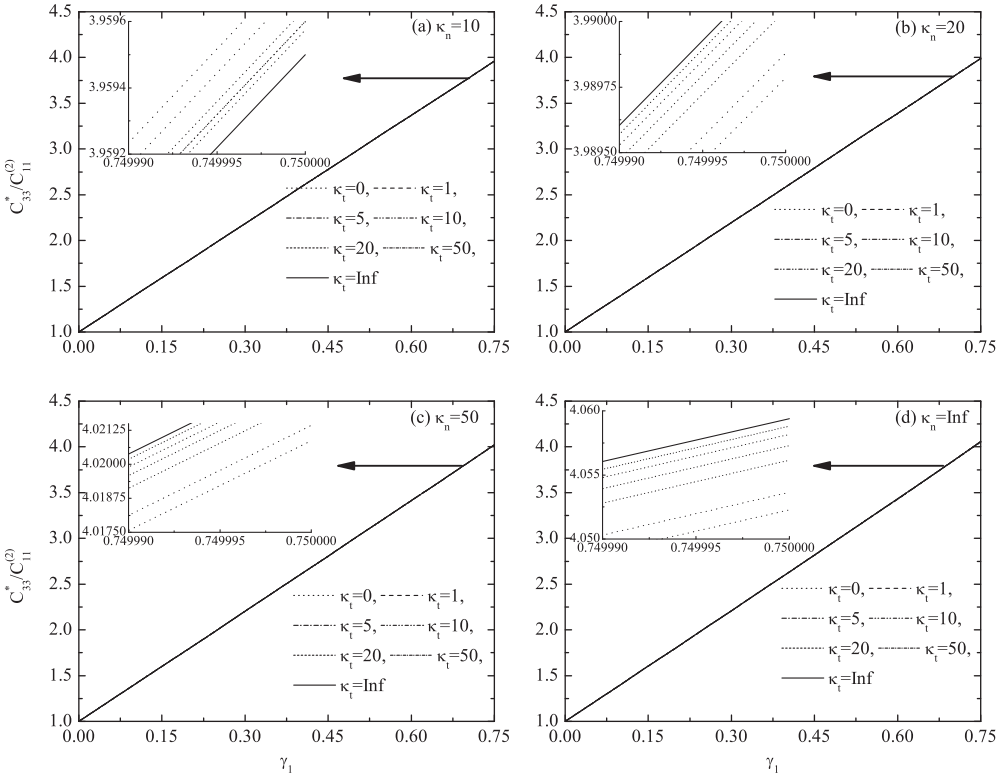

Fig. 7. Normalized effective coefficient $C^*_{33}/C^{(2)}_{11}$ versus fiber volume fraction γ_1 for different values of the imperfect parameters.

parameter. Meanwhile, the curves for $\kappa_n = \infty$ are increasing monotonic functions. Furthermore, the effective property gets softer as the tangential imperfect parameter κ_t increases and converges to the tangential perfect contact. Besides, the effective properties converge to the property for perfect contact as the imperfection parameter κ_t approaches to ∞. Numerical results has shown that the imperfection parameters (κ_t, κ_n) have a significant effect on the coefficient $C^*_{12}/C^{(2)}_{12}$ as well.

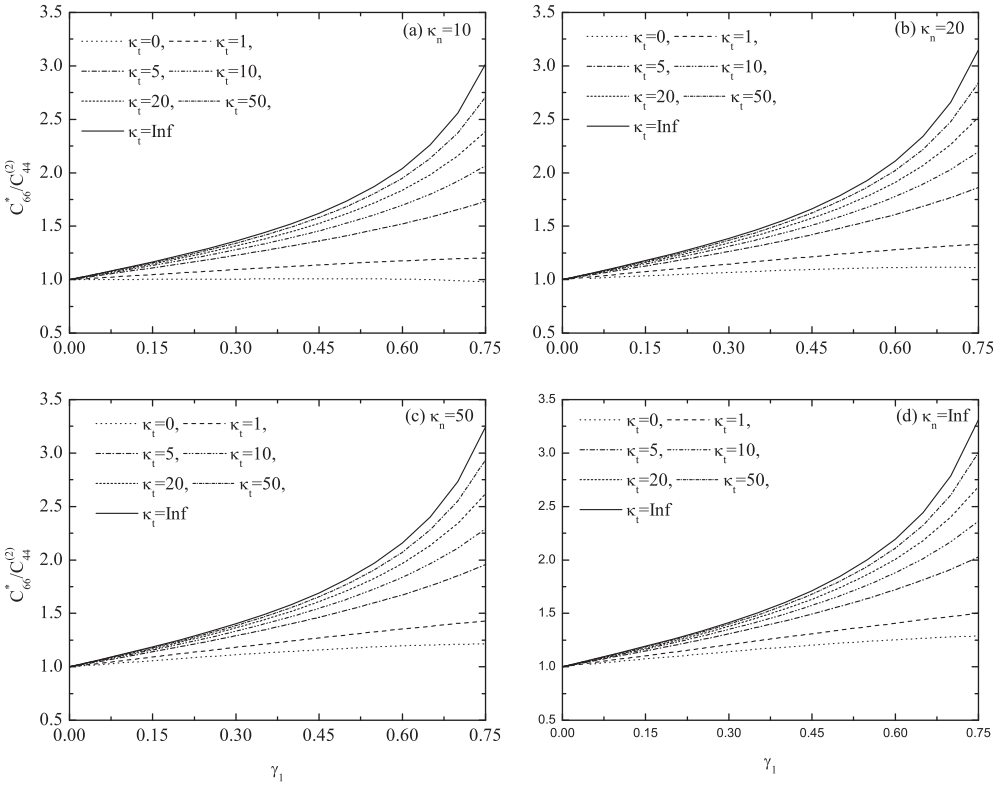

Fig. 8. Normalized effective coefficient $C^*_{66}/C^{(2)}_{44}$ versus fiber volume fraction γ_1 for different values of the imperfect parameters.

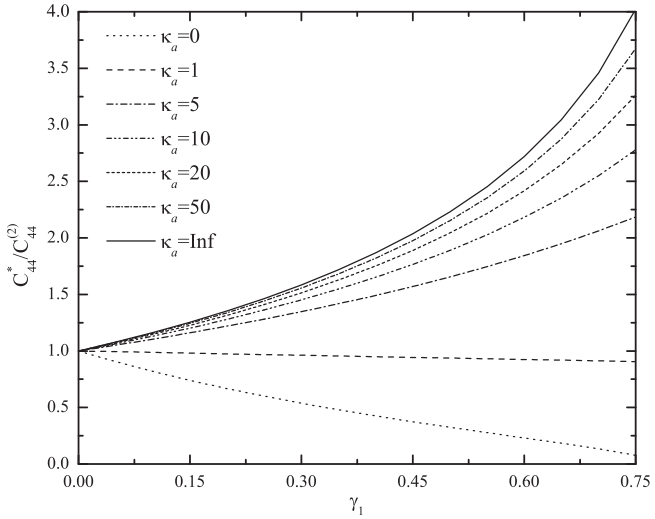

Fig. 9. Normalized effective coefficient $C^*_{44}/C^{(2)}_{44}$ versus fiber volume fraction γ_1 for different values of the axial imperfect parameter.

Figs. 6 and 7 report, the behavior of the normalized effective coefficients $C^*_{13}/C^{(2)}_{12}$ and $C^*_{33}/C^{(2)}_{11}$ with respect to the fiber volume fraction for different values of the tangential imperfect parameter $\kappa_t = 0; 1; 5; 10; 20; 50; \infty$ and some fixed normal imperfect parameters $\kappa_n = 10; 20; 50; \infty$. The curves apparently coincide but they are different for diverse choices of tangential imperfect values as can be seen in each figure. A linear behavior of the effective coefficient $C^*_{33}/C^{(2)}_{11}$ is remarkable where small influence of the normal and tangential imperfect parameters are observed. In contrast, slight curvature is perceived for $C^*_{13}/C^{(2)}_{12}$ where a significative (small) influence of the normal (tangential) imperfect parameter is noticed. In addition, the monotonic behavior of the curve in Fig. 6(a) ($\kappa_n = 10$) is different with respect to the remaining curves.

The behavior of the normalized effective coefficients $C^*_{66}/C^{(2)}_{44}$ with respect to the fiber volume fraction for different values of the tangential imperfect parameter $\kappa_t = 0; 1; 5; 10; 20; 50; \infty$ and some fixed normal imperfect parameters $\kappa_n = 10; 20; 50; \infty$ is presented in Fig. 8. In the whole range of the fiber volume fraction the curves are increasing and a moderate (significative) influence of the normal (tangential) imperfect parameter is reported. On the other hand, similar trend of the curves for the normalized effective coefficient $C^*_{44}/C^{(2)}_{44}$ can be observed in Fig. 9, for different values of the axial imperfect parameter $\kappa_a = 0; 1; 5; 10; 20; 50; \infty$. It can be noticed in the model that this coefficient does not depend on the normal imperfection parameter. Percolation limit for porous composites makes the shear effective property very small in comparison with the remaining curves at the same percolation regime. Numerical results have shown that the tangential imperfect parameter have a significant effect on the coefficient $C^*_{44}/C^{(2)}_{44}$.

The effective coefficients $C^*_{11}/C^{(2)}_{11}$, $C^*_{12}/C^{(2)}_{12}$, $C^*_{13}/C^{(2)}_{12}$, $C^*_{33}/C^{(2)}_{11}$, $C^*_{66}/C^{(2)}_{44}$ $\left(C^*_{44}/C^{(2)}_{44}\right)$ are analyzed in Fig. 10 with respect to the tangential (axial) imperfect parameter for different values of the normal imperfect parameter $\kappa_n = 10; 15; 20; 35; 50; 100; 500; 1000$ and for fiber volume fraction 0.45. The behavior of the effective coefficients depends on the imperfect parameters. For instance, the influence of the normal imperfect parameter is more evident for the effective coefficients $C^*_{11}/C^{(2)}_{11}, C^*_{12}/C^{(2)}_{12}$. Both coefficients

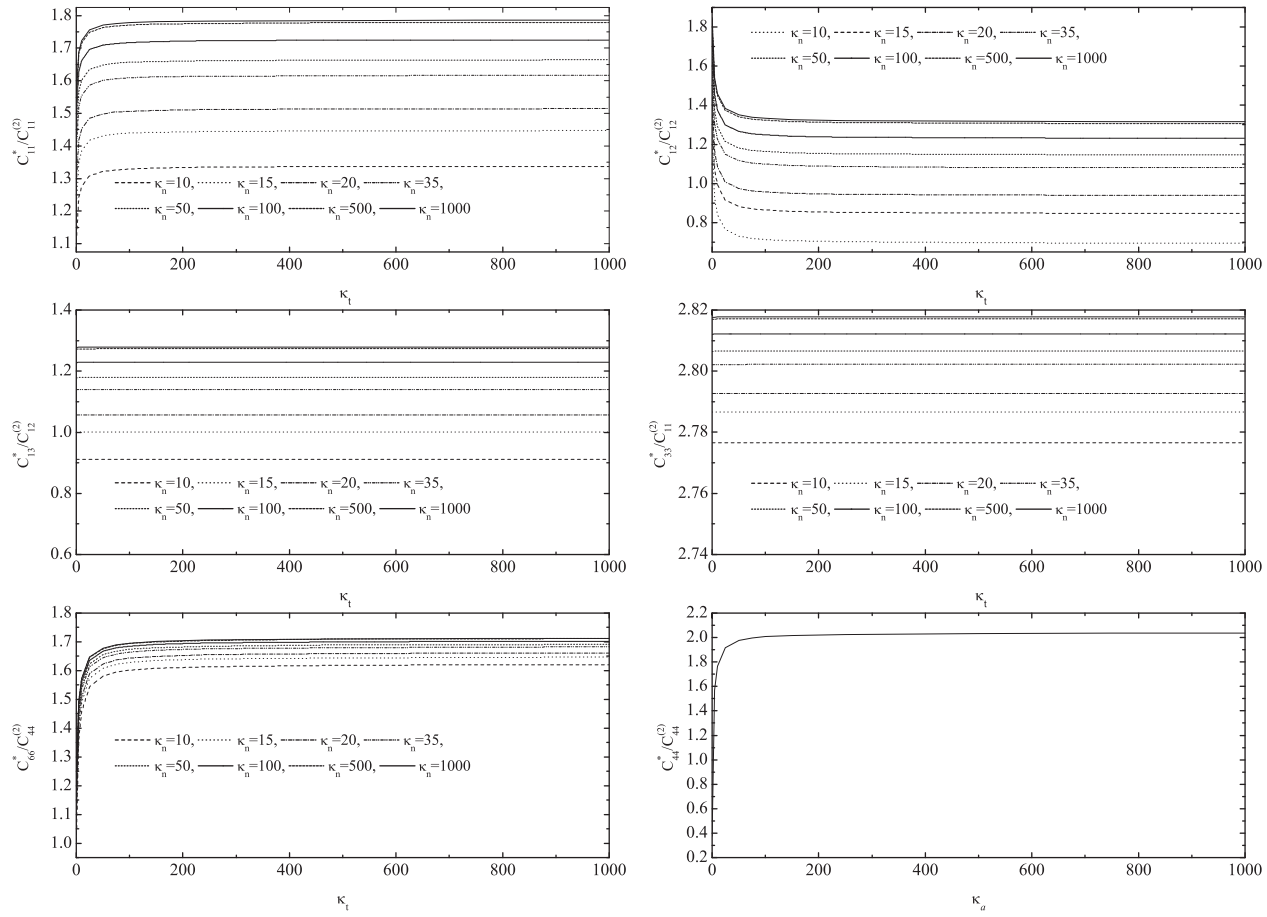

Fig. 10. Normalized effective coefficients $C^*_{11}/C^{(2)}_{11}$, $C^*_{12}/C^{(2)}_{12}$, $C^*_{13}/C^{(2)}_{12}$, $C^*_{33}/C^{(2)}_{11}$, $C^*_{66}/C^{(2)}_{44}$ $\left(C^*_{44}/C^{(2)}_{44}\right)$ versus tangential (axial) imperfect parameter for different values of the normal imperfect parameter and fiber volume fraction 0.45.

show the same trend for each value of the normal imperfect coefficient in the whole range of the tangential imperfect parameter. The overall coefficients $C^*_{13}/C^{(2)}_{12}$, $C^*_{33}/C^{(2)}_{11}$ do not qualitatively exhibit significant change with respect to the variation of the normal and tangential imperfect parameters. The normal imperfect parameters have a more reinforcement effect on the coefficient $C^*_{33}/C^{(2)}_{11}$ than on the coefficient $C^*_{13}/C^{(2)}_{12}$. In addition, the curves of $C^*_{66}/C^{(2)}_{44}$ are sketched and they are closer to the other ones in the whole range of κ_t variation.

6. Conclusion

This work dealt with the determination of the effective moduli of a periodic elastic composite material reinforced by straight parallel circular fibres, made of transversely isotropic material with axial, tangential and normal imperfect contacts at the interface. The investigation was carried out by adopting the semi-analytical method which is based on the finite element method and asymptotic homogenization approach. The present result was validated by means of comparison with limit cases and analytical expressions using the asymptotic homogenization method where the maximum error is very low. The results of the present work indicates the influence of imperfect adhesion on the effective moduli of composites with periodic elastic fibrous reinforcements.

Acknowledgments

The authors wish to acknowledge the CoNaCyT/México projects No. 129658, 82474 and the DGAPA UNAM/México project PAPIIT IN 119509-3. Thanks to Ramiro Chávez Tovar and Ana Pérez Arteaga for computational assistance.

References

Achenbach, J.D., Zhu, H., 1990. Effect of interphases on micro and macro mechanical behavior of hexagonal-array fiber composites. J. Appl. Mech. 57, 956–963.

Bakhvalov, N.S., Panasenko, G.P., 1989. Homogenization Averaging Processes in Periodic Media. Kluwer, Dordrecht.

Benveniste, Y., Miloh, T., 2001. Imperfect soft and stiff interfaces in two dimensional elasticity. Mech. Mater. 33, 309–323.

Guinovart-Diaz, R., Bravo-Castillero, J., Rodriguez-Ramos, R., Martinez-Rosado, R., Serrania, F., Navarrete, M., 2002. Modeling of elastic transversaly isotropic composite using the asymptotic homogenization method. Some comparisons with other models. Mater. Lett. 56 (6), 889–894.

Guinovart-Diaz, R., Rodriguez-Ramos, R., Bravo-Castillero, J., Sabina, F.J., Maugin, G.A., 2005. Closed-form thermo-elastic moduli of a periodic three-phase fiber-reinforced composite. J. Therm. Stress. 28, 1067–1093.

Hashin, Z., 1990. Thermoelastic properties of fiber composites with imperfect interface. Mech. Mater. 8, 333–338.

Hashin, Z., 1991a. The spherical inclusion with imperfect interface. J. Appl. Mech. 58, 444–449.

Hashin, Z., 1991b. Thermoelastic properties of particulate composites with imperfect interface. J. Mech. Phys. Solids 39, 745–762.

Hashin, Z., 2002. Thin interphase/imperfect interface in elasticity with application to coated fiber composites. J. Mech. Phys. Solids 50, 2509–2537.

Jasiuk, I., Tong, Y., 1989. The effect of interface on the elastic stiffness of composites. Mech. Compos. Mater. 100, 49–54.

Lopez-Realpozo, J.C., Rodriguez-Ramos, R., Guinovart-Diaz, R., Bravo-Castillero, J., Sabina, F.J., 2011. Transport properties in fibrous elastic rhombic composite with imperfect contact condition. Int. J. Mech. Sci. 53, 98–107.

Pobedrya, B.E., 1984. Mechanics of Composite Materials. Moscow State University Press, Moscow, in Russian.

Rodriguez-Ramos, R., Sabina, F.J., Guinovart-Diaz, R., Bravo-Castillero, J., 2001. Closed-form expressions for the effective coefficients of fibre-reinforced composite with transversely isotropic constituents-I. Elastic and square symmetry. Mech. Mater. 33, 223–235.

Sabina, F.J., Bravo-Castillero, J., Guinovart-Diaz, R., Rodriguez-Ramos, R., Valdiviezo-Mijangos, O.C., 2002. Overall behavior of two-dimensional periodic composites. Int. J. Solids Struct. 39 (2), 483–497.

Sanchez-Palencia, E., 1980. Non homogeneous media and vibration theory. Lecture Notes in Physics, vol. 127. Springer-Verlag, Berlin.

Zienkiewicz, O.C., Taylor, R.L., 2000. The Finite Element Method. The Basis, vol. 1. Butterworth-Heinemann, Oxford.